# An Effective CTL Peptide Vaccine for Ebola Zaire Based on Survivors' CD8+ Targeting of a Particular Nucleocapsid Protein Epitope with Potential Implications for COVID-19 Vaccine Design

Herst CV[a], Burkholz S[a], Sidney J[i], Sette A[i], Harris PE[g], Massey S[b], Brasel T[b], Cunha-Neto E[c,d,e], Rosa DS[d,f], Chao WCH[j], Carback R[a], Hodge T[a], Wang L[a], Ciotlos S[a], Lloyd P[a], Rubsamen R[a,h,*]

[a] *Flow Pharma, Inc., 3451 Vincent Road, Pleasant Hill, CA 94523*
[b] *University of Texas, Medical Branch,301 University Blvd, Galveston, TX 77555*
[c] *Laboratory of Clinical Immunology and Allergy-LIM60, University of São Paulo School of Medicine, São Paulo, Brazil*
[d] *Institute for Investigation in Immunology (iii) INCT, São Paulo, Brazil*
[e] *Heart Institute (Incor), School of Medicine, University of São Paulo, São Paulo, Brazil*
[f] *Department of Microbiology, Immunology and Parasitology, Federal University of São Paulo (UNIFESP/EPM), São Paulo, Brazil*
[g] *Endocrinology Division, Department of Medicine, School of Medicine, Columbia University, New York, New York, USA*
[h] *Massachusetts General Hospital, Department of Anesthesia, Critical Care and Pain Medicine, 55 Fruit St, Boston, MA 02114*
[i] *La Jolla Institute for Allergy and Immunology, 9420 Athena Circle La Jolla, CA 92037*
[j] *University of Macau, E12 Avenida da Universidade, Taipa, Macau, China*

---

**Abstract**

The 2013-2016 West Africa EBOV epidemic was the biggest EBOV outbreak to date. An analysis of virus-specific CD8+ T-cell immunity in 30 survivors showed that 26 of those individuals had a CD8+ response to at least one EBOV protein. The dominant response (25/26 subjects) was specific to the EBOV nucleocapsid protein (NP). It has been suggested that epitopes on the EBOV NP could form an important part of an effective T-cell vaccine for Ebola Zaire. We show that a 9-amino-acid peptide NP44-52 (YQVNNLEEI) located in a conserved region of EBOV NP provides protection against morbidity and mortality after mouse adapted EBOV challenge. A single vaccination in a C57BL/6

*Corresponding author
*Email address:* reidrubsamen@alum.mit.edu ( Rubsamen R)

mouse using an adjuvanted microsphere peptide vaccine formulation containing NP44-52 is enough to confer immunity in mice. Our work suggests that a peptide vaccine based on CD8+ T-cell immunity in EBOV survivors is conceptually sound and feasible. Nucleocapsid proteins within COVID-19 contain multiple class I epitopes with predicted HLA restrictions consistent with broad population coverage. A similar approach to a CTL vaccine design may be possible for that virus.

*Keywords:* Ebola Zaire vaccine, CTL Vaccine, controller, YQVNNLEEI, COVID-19, Flow Focusing

---

## 1. Introduction

Development of safe and effective vaccines for some viruses such as HIV and EBOV has been challenging [15]. Although vaccine development has been almost exclusively focused on eliciting a humoral immune response in the host through inoculation with whole protein antigen [40][54][46][24], CTL peptide vaccines producing a T cell response may offer an important alternative approach [19]. For HIV and EBOV and influenza in particular, the potential of CTL vaccines has been discussed [17][6][44]. Although computational prediction alone has been used for T-cell vaccine design [2][11], we saw a unique opportunity to see if a preventative EBOV T-cell vaccine could be successfully designed based on the specific epitopes targeted by survivors of documented EBOV infection.

The notion of HLA restricted HIV control has been described [45]. Pereyra-Heckerman conducted an analysis of virus-specific CD8+ T-cell immunity in individuals living with HIV [33]. They reported that HIV controllers, individuals living with HIV not undergoing treatment who do not progress to AIDS, have CD8+ cells targeting different HLA restricted class I epitopes on HIV compared with progressors, individuals with HIV who progress to AIDS in the absence of therapy. Pereyra-Heckerman suggested that this observation could guide the *in-silico* development of a CTL vaccine for HIV and other diseases.

Acquired immunity has been documented after EBOV infection [3]. Antibody as well as T-cell responses have been described [34]. Sakebe et al have shown that of 30 subjects surviving the 2013-2016 EBOV outbreak in West Africa, CD8+ T-cells from 26 of those survivors responded to at least one EBOV antigen, with 25 of the 26 responders targeting epitopes on EBOV NP [39]. One of the most commonly targeted EBOV eptitopes on EBOV NP in the survivor group (targeted by CD8+ cells from four survivors) was NP41-60 (IPVYQVNNLEEICQLIIQAF). They also suggested that a CTL vaccine for could be designed using epitopes targeted by CD8+ T-cells identified in these EBOV controllers.

Human pathogen-derived peptide antigens that are also recognized by C57BL/6 T cells have been previously described. These include peptides from vesicular stomatitis virus (VSV) RGYVYQGL [53], and human immunodeficiency virus (HIV) RGPGRAFVTI [4]. The existence of such epitopes makes possible a range of pre-clinical vaccine experiments without having to rely on non-human primates and expensive and complex-to-manage humanized mouse models. Wilson et al showed that the EBOV nucleoprotein (NP) is an immunogen that provides protective, CTL-mediated immunity against EBOV in a C57BL/6 mouse model and that this protection was conferred by a peptide sequence within Ebola Zaire: NP43-53 (VYQVNNLEEIC)[57]. Wilson et al came to this conclusion based on studying splenocytes harvested from mice vaccinated with Ebola Zaire NP using a Venezuelan equine encephalitis (VEE) vector. Their experiments showed that splenocytes from the vaccinated mice re-stimulated with NP43-53 had high levels of cytotoxic activity against target cells loaded with the EBOV NP peptide. Remarkably, NP43-53 also happens to be an 11 amino acid subsequence of the epitope identified by Sakebe et al, as most commonly favored for T-cell attack by survivors of the 2013-2016 EBOV outbreak in West Africa.

We set out to see if we could drive CTL expansion directed against NP43-53 to occur after vaccinating C57BL/6 mice with Ebola Zaire NP43-53 (VYQVNNLEEIC), and to subsequently conduct an *in-vivo* EBOV challenge study to see if this peptide was protective.

We fabricated adjuvanted microspheres for this study as a room temperature stable dry powder using the Flow Focusing process to be $11\mu M$ in diameter so as to prevent more than one microsphere from being phagocytosed by any given antigen presenting cell (APC) at the same time [29]. By loading only one peptide sequence per microsphere, we maximized the peptide payload and mitigated the possibility of multiple, different peptide sequences being delivered to the APC simultaneously, which could possibly result in competitive inhibition at the motif which could interfere with antigen presentation and subsequent T-cell expansion (Supplementary Material).

## 2. Results

We used a previously described biodegradable dry powder, PLGA microsphere, synthetic vaccine platform adjuvanted with TLR-4 and TLR-9 ligands [37] to immunize C57BL/6 mice with NP43-53 11-mer, the CTL+ class I peptide antigen from the Ebola Ziare NP protein identified by Wilson et al [57]. Microspheres containing NP43-53 and CpG were prepared as a dry powder formulation and suspended before use in a PBS injectate solution containing MPLA, and administered intradermally via injection at the base of the tail into mice as described in a previous publication [37]. Splenocytes from eight mice receiving the active vaccine, and eight mice receiving microspheres and adjuvants only, were harvested on day 14 and subjected to ELISPOT analysis evaluating $IFN-\gamma$ release in response to stimulation with the peptide used in the vaccination. As illustrated in Figure 1, there was no statistically significant difference between the ELISPOT data for the vaccinated mice *versus* the response seen in the negative control group.

Wilson reported that protection seen in her experiment was due to a peptide sequence within NP-43-53. We hypothesized that the NP43-53 epitope was inefficiently processed into MHC binding sub-sequences during antigen presentation. In order to explore possible H2-$D^b$ matches for peptide sequences contained within Ebola Zaire NP43-53 (VYQVNNLEEIC), we prepared three

9mer Subsequences of VYQVNNLEEIC
Evaluated for Immune Response

| Peptide Label | Peptide Sequence | Description |
|---|---|---|
| NP43-53 | VYQVNNLEEIC | Ebola Zaire NP 11mer peptide not H2-$D^b$ matched |
| NP43-51 | VYQVNNLEE | Sub-sequence 9mer VYQVNNLEEIC |
| NP44-52 | YQVNNLEEI | Sub-sequence 9mer VYQVNNLEEIC |
| NP45-53 | QVNNLEEIC | Sub-sequence 9mer VYQVNNLEEIC |

Table 1: Class I peptides used in the study. NP43-53 is the class I 11mer described by Wilson et al. which we found not to produce an immune response in a C57BL/6 mouse model. NP43-51, NP 44-52 and NP 45-53 are the three possible 9mer sub-sequences of NP43-53.

peptide vaccine formulations, each containing one of the three possible 9mer sub-sequences within NP43-53. These sequences are shown in Table 1. We then vaccinated, via intradermal (tail) injection, three groups of mice with microspheres containing one of the three 9mer sub-sequences of NP43-53 (6 per group). ELISPOT analysis was performed, stimulating harvested splenocytes with the three possible 9mer sub-sequences. Splenocytes from mice receiving the NP44-52 sub-sequence had a statistically higher ELISPOT response than mice vaccinated with the other two possible sub-sequence 9mers ($P < 0.0001$) as shown in Figure 2. This is consistent with the predicted H2-$D^b$ binding affinity of YQVNNLEEI as shown in Table 6.

We then loaded one population of adjuvanted microspheres with NP44-52 and a second population of adjuvanted microspheres loaded with VG19 from EBOV Zaire NP 273-291 (VKNEVNSFKAALSSLAKHG), a Class II epitope predicted to be relevant to NP43-53 based on the TEPITOPE algorithm using a technique described by Cunha-Neto at al [11]. This peptide has a predicted favorable H2-$I^b$ binding affinity as shown in Table 8.

We vaccinated 16 mice with those two populations of microspheres via intradermal (tail) administration and an 12 additional mice with two populations of

microspheres, one population containing NP43-53 and the other VG19. $IFN-\gamma$ release as quantified by ELISPOT after the spleens were harvested on day 14 after immunization showed that the immune response to the 9mer NP44-52 was higher than the immune response after vaccination with NP43-53 and that this difference was statistically significant ($P < 0.0001$) Figure 3.

We conducted a pilot study demonstrating that intraperitoneal injection produced a statistically superior immune response by ELISPOT compared with intradermal tail injection in C57BL/6 mice (Supplementary Material). Based on the data from that study, we chose to proceed with intraperitoneal administration for the challenge portion of this study.

We dosed three groups of mice, ten mice per group, with the adjuvanted microsphere vaccine formulation containing NP44-52 and VG-19, with each peptide in a distinct microsphere population, and challenged these mice 14 days after vaccine administration with escalating IP administered doses of mouse adapted EBOV (maEBOV) (Group 3 - 100 PFU, Group 5 - 1000 PFU and Group 7 - 10,000 PFU). The composition of the vaccine used for the exposure study is described in Supplementary Material. A second set of three control groups of mice (groups 2, 4 and 6), ten mice per group (mock groups), received PBS buffer solution alone and served as control animals for the study and were similarly challenged with maEBOV. Group 1 animals served as study controls and received no PBS buffer, vaccine or maEBOV injections. All mice were sourced from Jackson Labs and were 6-8 weeks of age and 15-25 grams at the time of vaccination. The dosing regimen is outlined in Table 2.

Peak mortality across all groups tested was seen in mice challenged with 1,000 PFU maEBOV *versus* PBS buffer control as shown in the survival curve in Figure 5. Clinical observation data shown in Figure 6 and Figure 7 and daily weight data shown in Figure 8 and Figure 9 show protection from morbidity in all active vaccinated mice exposed to 1,000 PFU maEBOV.

PBS buffer mock-vaccinated mice showed mortality increasing from the 100 PFU to 1,000 PFU as shown in Figure 10a and Figure 5. We saw a paradoxical effect in control animals with survival increasing between 1,000PFU (Figure 5)

and 10,000 PFU (Figure 11a). We believe this was caused by innate immunity triggered by the very large maEBOV challenge. All mice in all vaccinated groups across both experiments survived and showed no morbidity by clinical observation scores and weight data.

For each of the three challenge levels, the difference between the number of survivors in the vaccinated group *versus* the PBS control group was statistically significant by chi square (100 PFU P = 0.001; 1000 PFU P = 0.0003; 10,000 PFU P = 0.003)

Serum samples from sacrificed animals exposed to EBOV who did not receive vaccine were quantitatively assayed for various cytokines using BioPlex plates. Animals having unwitnessed demise did not have serum samples collected. A Pearson Correlation Analysis was performed to assess relationships between specific cytokine levels and survival. The results are shown in Table 4.

We observed low levels of IL-6 in surviving mice. NHPs infected with EBOV have been determined by other researchers to have elevated levels of IL-6 in plasma and serum [23][14]. EBOV infected humans have also shown elevated IL-6 levels and these elevated levels have been associated with increased morality [56].

Similarly, we observed low levels of MCP-1, IL-9 and GM-CSF in survivors. Increased serum and plasma levels of MCP-1 have been observed in EBOV infected NHPs [18][23][14] and elevated levels of MCP-1 were associated with fatalities in EBOV infected human subjects [56]. Human survivors of EBOV have been found to have very low levels of circulating cytokines IL-9 and elevated levels of GM-CSF have been associated with fatality in humans exposed to EBOV [56].

We saw increased levels of $IFN-\gamma$ in survivors. Other vaccine studies have associated $IFN-\gamma$ with protection [55][30].

## Dosing Table

## Vaccinated Animals *versus* PBS Controls
## 100, 1000, and 10,000 PFU maEBOV Challenge

| Group | N | Active / Control | Formulation | Route | Challenge |
|---|---|---|---|---|---|
| 1 | 4 | Control | N/A | N/A | N/A |
| 2 | 10 | Control | PBS | 400$\mu$l IP | 100PFU maEBOV |
| 3 | 10 | Active | 10mg Adjuvanted Microspheres with NP44-52<br>10mg Adjuvanted Microspheres with VG-19 | 400$\mu$l IP | 100 PFU maEBOV |
| 4 | 10 | Control | PBS | 400$\mu$l IP | 1,000PFU maEBOV |
| 5 | 10 | Active | 10mg Adjuvanted Microspheres with NP44-52<br>10mg Adjuvanted Microspheres with VG-19 | 400$\mu$l IP | 1,000 PFU maEBOV |
| 6 | 10 | Control | PBS | 400$\mu$l IP | 10,000PFU maEBOV |
| 7 | 10 | Active | 10mg Adjuvanted Microspheres with NP44-52<br>10mg Adjuvanted Microspheres with VG-19 | 400$\mu$l IP | 10,000 PFU maEBOV |

Table 2: C7BL/6 maEBOV challenge study dosing regimen with PBS (buffer) controls. All challenges were done with Ebola virus M. musculus/COD/1976/Mayinga-CDC-808012 (maEBOV) delivered IP. Mice in Group 1 received no injections.

## Mouse Observation Clinical Scores

| Scale | Description of Animal |
|---|---|
| 1 | Healthy |
| 2 | Lethargic and/or ruffled fur<br>(triggers a second observation) |
| 3 | Ruffled fur, lethargic and hunched posture, orbital tightening<br>(triggers a third observation) |
| 4 | Ruffled fur, lethargic, hunched posture, orbital tightening<br>reluctance to move when stimulated, paralysis or greater than 20% weight loss<br>(requires immediate euthanasia) |

Table 3: Clinical score indices used to track morbidity in study animals.

## 3. Summary and Discussion

Most preventative vaccines are designed to elicit a humoral immune response, typically via the administration of whole protein from a pathogen. In contrast, a T-cell vaccine is meant to elicit a cellular immune response directing CD8+ cells to expand and attack cells presenting the HLA Class I restricted pathogen-derived peptide antigen. Difficulty in obtaining a reliable immune response from peptide antigens and the HLA restricted nature of CTL vaccines have limited their utility to protect individuals from infectious disease [59]. However, observations derived from individuals able to control HIV infection [33] and EBOV infection [39] demonstrating that control may be associated with specific CTL targeting behavior, suggest that there may be an important role for HLA restricted peptide vaccines for protection against infectious disease for which development of an effective traditional whole protein vaccine has proved to be difficult. The adjuvanted microsphere peptide vaccine platform described here incorporates unmodified peptides making possible rapid manufacture and deployment to respond to a new viral threat.

NP44-52 is located within one of the EBOV nucleocapsid proteins considered essential for virus replication. This epitope resides in a sequence conserved across multiple EBOV strains as shown in Figure 12. A 7.3Å structure for NP and VP24 is shown for context in Figure 13a [52]. A 1.8Å resolution structure rendering for EBOV NP shown in Figure 13b illustrates that NP44-52 is a buried structural loop, which is likely to be important to the structural integrity of the EBOV NP protein [13]. This structural role of NP44-52 likely explains its conservation across EBOV strains.

CTL targeting of the EBOV NP protein has been described [38][20]. Nucleocapisid proteins are essential for EBOV replication [48]. Recent advances in T-cell based vaccines have focused on avoiding all variable viral epitopes and incorporating only conserved regions [6][21]. EBOV NP may more conserved than nucleocapsid proteins VP35 and VP24 making it more suitable as a CTL vaccine target [7][57]. The nucleocapsid proteins in SARS-CoV are also essential for

that virus to function normally [8]. This suggests that a CTL vaccine targeting coronavirus nucleocapsid could be effective against SARS-CoV or COVID-19.

We have shown that an H2-$D^b$ restricted Class I peptide exists within the NP41-60 epitope identified by Sakebe et al as the most commonly favored NP epitope for CD8+ attack by survivors of the 2013-1016 EBOV outbreak in West Africa. We have demonstrated, when delivered in conjunction with a predicted-matched Class II epitope using an adjuvanted microsphere peptide vaccine platform, NP44-52 protection against mortality and morbidity for the maEBOV challenge doses tested in a C57BL/6 mouse model. We accomplished this with an adjuvanted, microsphere-based, synthetic CTL peptide vaccine platform producing a protective immune response 14 days after a single administration.

We saw what appears to be an innate immune response at the 10,000 PFU EBOV exposure level. It has been suggested that EBOV can mediate an innate immunity response through stimulation of TLR-4 [28]. Because the adjuvanted microsphere vaccine used in this experiment incorporates a TLR-4 agonist, we dosed 10 mice with adjuvanted microspheres without peptides and found the level of protection after exposure to 100 PFU EBOV to be statistically no different from that seen in PBS buffer controls. We conclude that level of protection conferred by the adjuvanted vaccine described in this study is dependant on delivering peptides with the microspheres.

EBOV can cause severe pulmonary problems in exposed subjects [31]. These problems can be especially severe when the virus is delivered by aerosol [12] [26]. Interaction of EBOV specific antibody, NHP lung tissue and EBOV delivered to NHPs via aerosol can produce a more lethal effect than in NHPs without circulating anti-EBOV antibody exposed to aerosolized EBOV (unpublished conference presentation). This suggests that a CTL vaccine may be more effective for prophylaxis against filovirus protection than an antibody vaccine if the anticipated route of EBOV exposure is via aerosol.

Sakebe et al identified A*30:01:01 as the only HLA type common to all four survivors in their study with CD8+ targeting of NP41-60. The A*30 supertype is relatively common in West Africa: 13.3% for Mali, 15.4% for Kenya,

16.3% for Uganda, and 23.9% for Mozambique [27]. Although peptide vaccines are by their nature HLA restricted, it may be possible to create a CTL vaccine directed against EBOV for use alone or in conjunction with a whole protein vaccine to produce an antibody response in tandem, by incorporating additional Class I peptides from epitopes targeted by controllers to broaden the HLA coverage of the vaccine. MHC binding algorithms hosted by the IEDB predict that YQVNNLEEI will bind strongly to the MHC of HLA-A*02:06, HLA-A*02:03 and HLA-A*02:01 individuals (Table 5)[51]. HLA-DR binding database analysis also suggests that VKNEVNSFKAALSSLAKHG demonstrates sufficiently promiscuous binding characteristics cover that same population (Table 7)[51]. Taken together, a peptide vaccine based on YQVNNLEEI and VKNEVNSFKAALSSLAKHG could produce a cellular immune response in about 50% of the population of the Sudan and about 30% of the population of North America.

This same approach could be applied to COVID-19 which also has conserved regions in nucleocapsid proteins as shown in Figure 14 and Figure 15. Antigenic escape allows a virus to retain fitness despite an immune response to vaccination [16]. Picking conserved regions for vaccine targeting is an important part of mitigating this problem. Coronavirus spike protein, for example, may be particularly susceptible to mutation meaning that antigenic escape would be likely if the spike protein was targeted by a coronavirus vaccine, making it difficult to achieve durable protection[58].

We took all possible 424 9mer peptide sequences from the COVID-19 nucleocapsid protein sequences available and evaluated each peptide for HLA restriction using NetMHC 4.0 and NetMHCpan 4.0 [51][25][1]. We analyzed 9mer peptide sequences because these are often associated with superior MHC binding properties than class I peptides of other lengths [49]. We found 53 unique peptides with predicted binding below 500nM from NetMHC 4.0 and/or NetMHCpan 4.0. These results are shown in Table 9, Table 10, Table 11 and Table 12.

We proceeded to determine the predicted HLA population coverage of a vaccine incorporating all 53 peptides using median values of the ANN, SMM, NetMHC 4.0 and NetMHCpan 4.0 algorithms hosted by IEDB [51]. These 53

peptides, taken together, had predicted HLA coverage of greater than 97% of the world's population as shown in Table 14. We also calculated HLA coverage based on alleles specific to populations in China and found that coverage across those individuals could be expected to be within 3% percent of the world wide coverage estimate as shown in Table 15. This same population coverage could be achieved with 16 of the 53 unique peptides as shown in Table 13.

Seven of the 53 peptides with a predicted HLA match have been tested *in-vitro* for HLA binding affinity by various researchers [51]. These binding affinity assays were originally performed with the SARS virus during a previous outbreak. Specific literature references for these *in-vitro* assays for each peptide sequence are as follows: ASAFFGMSR, LSPRWYFYY, QQQGQTVTK: [42], FPRGQGVPI: [42][22][36][47], GMSRIGMEV: [22][50][10][32][9], KTFPPTEPK: [42][22][35][47][5] and LLLDRLNQL: [32][10][9][50][60]. These seven peptides are shown in red in Table 9, Table 10 and Table 13.

The remaining 46 COVID-19 peptides listed in could also be further qualified as potential vaccine candidates by confirming MHC binding predictions by *in-vitro* binding affinity and/or binding stability studies [43][41][22]. Another approach to evaluating the 53 COVID-19 candidate vaccine peptides though *in-vitro* testing is also possible.

As we have shown in this paper, a peptide targeted by EBOV controllers could form the basis of a preventative vaccine for EBOV. ELISPOT analysis of PBMCs taken from the peripheral blood of COVID-19 controllers and progressors to assess the presence of a differential response to the 53 peptides could lead to a broadly applicable protective CTL vaccine against COVID-19 by incorporating peptides into the vaccine that are more commonly targeted for CD8+ attack by the controllers *versus* the progressors. The extent of the COVID-19 outbreak should allow many more controllers to be identified then the 30 individuals studied by Sakabe. Furthermore, Sakebe did not report progressor data perhaps because of the difficulty in obtaining blood samples from those patients. If researchers act now during the COVID-19 outbreak, perhaps controller and progressor blood samples could be collected and prospectively analyzed, quickly

creating a database of optimal candidate class I peptides for inclusion into a CTL vaccine with potentially broad HLA coverage for subsequent rapid manufacture and deployment. It would be interesting to see the extent to which the peptides favored by controllers appear on COVID-19 nucleocapsid, making COVID-19 a second example, across two different viruses, of controllers exhibiting CTL attack preferentially on the nucleocapsid protein.

## 4. Acknowlegements

All animal handling was done in accordance with NIH and institutional animal care and use guidelines by Aragen Bio-sciences in Morgan Hill California and the University of Texas, Medical Branch, Galveston Texas working in conjunction with the Galveston National Laboratory. The research was funded by Flow Pharma, Inc.

## 5. Declaration of Interest Statement

CV Herst, Scott Burkholz, Lu Wang, Peter Lloyd and Reid Rubsamen are employees of Flow Pharma, Inc. all receiving cash and stock compensation. Alessandro Sette, Paul Harris, William Chao and Tom Hodge are members of Flow Pharmas Scientific Advisory Board. Alessandro Sette and Paul Harris have received cash and stock compensation as SAB members. Richard Carback and Serban Ciotlos are consultants to Flow Pharma, both receiving cash and stock compensation. John Sidney works with Alessandro Sette at the La Jolla Institute of Allergy and Immunology. Flow Pharma, Inc. has previously contracted with the La Jolla Institute of Allergy and Immunology to support other research not related to this study funded under STTR contract CBD18-A-002-0016. Reid Rubsamen, CV Herst, Scott Burkholz, Lu Wang, Peter Lloyd, Richard Carback, Serban Ciotlos and Tom Hodge are named inventors on various issued and pending patents relating to Flow Pharma's technology. All of the rights to all of these patents have been assigned by each of the inventors to

Flow Pharma. Shane Massey, Trevor Brasel, Edecio Cunha-Neto and Daniela Rosa have nothing to declare.

## References


[1] Massimo Andreatta and Morten Nielsen. Gapped sequence alignment using artificial neural networks: application to the mhc class i system. *Bioinformatics*, 32(4):511–517, 2016. URL https://doi.org/10.1093/bioinformatics/btv639.

[2] Mekibib B and Arilen K. Aerosol transmission of filoviruses. *Viruses*, 9(5): 148, May 2016. doi: 10.3390/v8050148. URL https://doi.org/10.3390/v8050148.

[3] Steve E Bellan, Juliet R C Pulliam, Jonathan Dushoff, and Lauren Ancel Meyers. Ebola control: effect of asymptomatic infection and acquired immunity. *The Lancet*, 384(9953):1499–1500, October 2014. doi: 10.1016/S0140-6736(14)61839-0. URL https://doi.org/10.1016/S0140-6736(14)61839-0.

[4] R Billeskov, Y Wang, S Solaymani-Mohammadi, B Frey, S Kulkarni, P Andersen, E Marie Agger, Y Sui, and J Berzofsky. Low antigen dose in adjuvant-based vaccination selectively induces cd4 t cells with enhanced functional avidity and protective efficacy. *J Immunol*, 198(9):3494–3506, 2017. doi: 10.4049/jimmunol.1600965. URL https://doi.org/10.4049/jimmunol.1600965.

[5] Thomas Blicher, Jette Sandholm Kastrup, Soren Buus, and Michael Gajhede. High-resolution structure of hla-a* 1101 in complex with sars nucleocapsid peptide. *Acta Crystallographica Section D: Biological Crystallography*, 61(8):1031–1040, 2005. doi: 10.1107/S0907444905013090.

[6] N. Borthwick, T. Ahmed, B. Ondondo, P. Hayes, A. Rose, U. Ebrahimsa, E. J. Hayton, A. Black, A. Bridgeman, M. Rosario, A.V. Hill, E. Berrie,

E. Moyle, N. Frahm, J. Cox, S. Colloca, A. Nicosia, J. Gilmour, A.J. McMichael, L. Dorrell, and L. Hanke. Vaccine-elicited human t cells recognizing conserved protein regions inhibit hiv-1. *Mol Ther.*, 22(2):464–475, 2014. doi: 10.1038/mt.2013.248. URL https://doi.org/10.1038/mt.2013.248.

[7] BaslerGaya CF and Amarasinghe K. Evasion of interferon responses by ebola and marburg viruses. *Journal of Interferon & Cytokine Research*, 29 (9), September 2009. doi: 10.1089/jir.2009.0076. URL https://doi.org/10.1089/jir.2009.0076.

[8] Chung-ke Chang, Ming-Hon Hou, Chi-Fon Chang, Chwan-Deng Hsiao, and Tai-huang Huang. The sars coronavirus nucleocapsid protein–forms and functions. *Antiviral research*, 103:39–50, 2014. URL https://doi.org/10.1016/j.antiviral.2013.12.009.

[9] Ying-Kit Cheung, Samuel Chak-Sum Cheng, Fion Wan-Yee Sin, Kin-Tak Chan, and Yong Xie. Induction of t-cell response by a dna vaccine encoding a novel hla-a* 0201 severe acute respiratory syndrome coronavirus epitope. *Vaccine*, 25(32):6070–6077, 2007. URL https://doi.org/10.1016/j.vaccine.2007.05.025.

[10] YK Cheung, SC Cheng, FW Sin, KT Chan, and Y Xie. Investigation of immunogenic t-cell epitopes in sars virus nucleocapsid protein and their role in the prevention and treatment of sars infection. *Hong Kong medical journal= Xianggang yi xue za zhi*, 14:27–30, 2008.

[11] E Cunha-Neto, DS Rosa, PE Harris, T Olson, A Morrow, A Ciotlos, CV Herst, and RM Rubsamen. An approach for a synthetic ctl vaccine design against zika flavivirus using class i and class ii epitopes identified by computer modeling. *Frontiers in Immunology*, 2017. doi: doi.org/10.3389/fimmu.2017.00640. URL https://doi.org/10.3389/fimmu.2017.00640.

[12] Alves DA, Glynn AR, Steele KE, Lackemeyer MG, Garza NL, Buck JG, Mech C, and Reed DS. Aerosol exposure to the angola strain of marburg virus causes lethal viral hemorrhagic fever in cynomolgus macaques. *Veterinary Pathology*, 2010. doi: 10.1177/0300985810378597.

[13] Shishang Dong, Peng Yang, Guobang Li, Baocheng Liu, Wenming Wang, Xiang Liu, Boran Xia, Cheng Yang, Zhiyong Lou, Yu Guo, and Zihe Rao. Insight into the ebola virus nucleocapsid assembly mechanism: crystal structure of ebola virus nucleoprotein core domain at 1.8 å resolution. *Protein & Cell*, 6(5):351–362, May 2015. ISSN 1674-8018. doi: 10.1007/s13238-015-0163-3. URL https://doi.org/10.1007/s13238-015-0163-3.

[14] H. Ebihara, B. Rockx, A. Marzi, F. Feldmann, E. Haddock, D. Brining, R.A. LaCasse, D. Gardner, and H. Feldmann. Host response dynamics following lethal infection of rhesus macaques with zaire ebolavirus. *J. Infect. Dis.*, 204:S991–S999, 2011. doi: DOI: 10.1093/infdis/jir336.

[15] Heinz Feldmann, Steven Jones, Hans-Dieter Klenk, and Hans-Joachim Schnittler. Ebola virus: from discovery to vaccine. *Nature Reviews Immunology*, 3:677–685, August 2003. doi: 10.1038/nri1154. URL https://doi.org/10.1038/nri1154.

[16] Steven A Frank and Robin M Bush. Barriers to antigenic escape by pathogens: trade-off between reproductive rate and antigenic mutability. *BMC evolutionary biology*, 7(1):229, 2007. URL https://doi.org/10.1186/1471-2148-7-229.

[17] Rezza G. A vaccine against ebola: Problems and opportunities. *Human Vaccines and Immunotherapeutics*, 11(5):1258–1260, 2014. doi: 10.1080/21645515.2015.1021528. URL https://doi.org/10.1080/21645515.2015.1021528.

[18] T.W. Geisbert, L.E. Hensley, T. Larsen, H.A. Young, D.S. Reed, J.B. Geisbert, D.P. Scott, E. Kagan, and K.J. Jahrling, P.B.; Davis. Pathogenesis

of ebola hemorrhagic fever in cynomolgus macaques: Evidence that dendritic cells are early and sustained targets of infection. *Am. J. Pathol.*, 163: 2347–2370, 2003. doi: DOI: 10.1016/S0002-9440(10)63591-2.

[19] S.C. Gilbert. T-cell-inducing vaccines - what's the future? *Immunology*, 135(1):19–26, 2012. doi: 10.1111/j.1365-2567.2011.03517.x. URL https://doi.org/10.1111/j.1365-2567.2011.03517.x.

[20] Manisha Gupta, Patricia Greer, Siddhartha Mahanty, Wun-Ju Shieh, Sherif R. Zaki, Rafi Ahmed, and Pierre E. Rollin. Cd8-mediated protection against ebola virus infection is perforin dependent. *Journal of Immunology*, 174(7):4198–4202, April 2005. doi: 10.4049/jimmunol.174.7.4198. URL https://doi.org/10.4049/jimmunol.174.7.4198.

[21] Scott G. Hansen, Julia C. Ford, Matthew S. Lewis, Abigail B. Ventura, Colette M. Hughes, Lia Coyne-Johnson, Nathan Whizin, Kelli Oswald, Rebecca Shoemaker, Tonya Swanson, Alfred W. Legasse, Maria J. Chiuchiolo, Christopher L. Parks, Michael K. Axthelm, Jay A. Nelson, Michael A. Jarvis, Michael Piatak, Jeffrey D. Lifson, and Louis J. Picker. Profound early control of highly pathogenic siv by an effector memory t-cell vaccine. *Nature*, 473:523–527, May 2011. doi: 10.1038/nature10003. URL https://doi.org/10.1038/nature10003.

[22] Mikkel Harndahl, Kasper Lamberth, Sune Justesen, Gustav Rder, Michael Madsen, Christina Sylvester-Hvid, Morten Nielsen, Claus Lundegaard, Mette Voldby Larsen, Sheila Tang, Sren Brunak, Ole Lund, and Sren Buus. Large scale analysis of peptide-hla class i interactions. *IEDB*, 2006. URL https://www.iedb.org/reference/1000945.

[23] L.E.. Hensley, H.A. Young, P.B. Jahrling, and T.W. Geisbert. Proinflammatory response during ebola virus infection of primate models: Possible involvement of the tumor necrosis factor receptor superfamily. *Immunol. Lett.*, 80:169–179, 2002. URL https://www.ncbi.nlm.nih.gov/pubmed/11803049.

[24] Steven M Jones, Heinz Feldmann, Ute Ströher, Joan B Geisbert, Lisa Fernando, Allen Grolla, Hans-Dieter Klenk, Nancy J Sullivan, Viktor E Volchkov, Elizabeth A Fritz, Kathleen M Daddario, Lisa E Hensley, Peter B Jahrling, and Thomas W Geisbert. Live attenuated recombinant vaccine protects nonhuman primates against ebola and marburg viruses. *Nature Medicine*, 11:786–790, June 2005. doi: 10.1038/nm1258. URL https://doi.org/10.1038/nm1258.

[25] Vanessa Jurtz, Sinu Paul, Massimo Andreatta, Paolo Marcatili, Bjoern Peters, and Morten Nielsen. Netmhcpan-4.0: improved peptide–mhc class i interaction predictions integrating eluted ligand and peptide binding affinity data. *The Journal of Immunology*, 199(9):3360–3368, 2017. URL https://doi.org/10.4049/jimmunol.1700893.

[26] Leffel K and Reed D. Marburg and ebola viruses as aerosol threats. *Biosecurity and Bioterrorism: Biodefense Strategy, Practice, and Science*, 2(3), September 2004. doi: 10.1089/bsp.2004.2.186.

[27] I Kalidi, Y Fofana, A A Rahly, V Bochu, C Dehay, J Gony, and J Hors. Study of hla antigens in a population of mali (west africa). *Tissue Antigens*, 31:98–102, 03 1988. URL https://www.ncbi.nlm.nih.gov/pubmed/3163860.

[28] Chih-Yun Lai, Daniel P Strange, Teri Ann S Wong, Axel T Lehrer, and Saguna Verma. Ebola virus glycoprotein induces an innate immune response in vivo via tlr4. *Frontiers in microbiology*, 8:1571, 2017. URL https://doi.org/10.3389/fmicb.2017.01571.

[29] LF Martin-Banderas, M Flores-Mosquera, P Riesco-Chueca, A Rodriguez-Gil, A Cebolla, and S Chávez. Flow focusing: a versatile technology to produce size-controlled and specific-morphology microparticles. *Small*, 4, 2005. doi: 10.1002/smll.200500087.

[30] A.K. McElroy, R.S. Akondy, C.W. Davis, A.H. Ellebedy, A.K. Mehta, C.S. Kraft, G.M. Lyon, B.S. Ribner, J. Varkey, and J. Sidney. Human ebola

virus infection results in substantial immune activation. *Proc. Natl. Acad. Sci.*, 1122:4719–4724, 2015. doi: doi: 10.1073/pnas.1502619112.

[31] Charles K. Nfon, Anders Leung, Greg Smith, Carissa Embury-Hyatt, Gary Kobinger, and Hana M. Weingartl. Immunopathogenesis of severe acute respiratory disease in zaire ebolavirus-infected pigs. *PLoS ONE*, 2013. doi: 10.1371/journal.pone.0061904.

[32] Satoshi Ohno, Shunsuke Kohyama, Maiko Taneichi, Osamu Moriya, Hidenori Hayashi, Hiroshi Oda, Masahito Mori, Akiharu Kobayashi, Toshitaka Akatsuka, Tetsuya Uchida, et al. Synthetic peptides coupled to the surface of liposomes effectively induce sars coronavirus-specific cytotoxic t lymphocytes and viral clearance in hla-a* 0201 transgenic mice. *Vaccine*, 27(29): 3912–3920, 2009. URL https://doi.org/10.1016/j.vaccine.2009.04.001.

[33] F Pereyra, D Heckerman, J M Carlson, C. Kadie, D Z Soghoian, D Karel, A Goldenthal, O B. Davis, C E DeZiel, and T Lin. Hiv control is mediated in part by cd8+ t-cell targeting of specific epitopes. *J Virol*, 88:12937–12948, 2014. doi: 10.1128/JVI.01004-14. URL https://doi.org/10.1128/JVI.01004-14.

[34] Julia Ponomarenko, Kerrie Vaughan, Sinu Paul, Bjoern Peters, Alessandro Sette, Maximilian Haeussler, and Sebastian Maurer-Stroh. Ebola: an analysis of immunity at the molecular level. *IEEE*, July 2015. doi: https://doi:10.1109/aisw.2015.7469230. URL https://doi:10.1109/aisw.2015.7469230.

[35] Michael Rasmussen, Mikkel Harndahl, Anne Bregnballe Kristensen, Ida Kallehauge Nielsen, Kasper W Jorgensen, Anette Stryhn, Morten Nielsen, and Sren Buus. Large scale analysis of peptide - hla-i stability. *IEDB*, 2014. URL https://www.iedb.org/reference/1028287.

[36] Michael Rasmussen, Mikkel Harndahl, Anne Bregnballe Kristensen, Ida Kallehauge Nielsen, Kasper W Jorgensen, Anette Stryhn, Morten

Nielsen, and Sren Buus. Large scale analysis of peptide - hla-i stability. *IEDB*, 2014. URL https://www.iedb.org/reference/1028291.

[37] R. M. Rubsamen, C. V. Herst, P. M. Lloyd, and D. E. Heckerman. Eliciting cytotoxic t-lymphocyte responses from synthetic vectors containing one or two epitopes in a c57bl/6 mouse model using peptide-containing biodegradable microspheres and adjuvants. *Vaccine*, 32:4111–4116, 2014. doi: 10.1016/j.vaccine.2014.05.071. URL https://doi.org/10.1016/j.vaccine.2014.05.071.

[38] Jain S and Baranwal M. Conserved peptide vaccine candidates containing multiple ebola nucleoprotein epitopes display interactions with diverse hla molecules. *Medical Microbiology and Immunology*, 208(2):227–238, April 2019. doi: 10.1007/s00430-019-00584-y. URL https://doi.org/10.1007/s00430-019-00584-y.

[39] Saori Sakabe, Brian M. Sullivan, Jessica N. Hartnett, Refugio Robles-Sikisaka, Karthik Gangavarapu, Beatrice Cubitt, Brian C. Ware, Dylan Kotliar, Luis M. Branco, Augustine Goba, Mambu Momoh, John Demby Sandi, Lansana Kanneh, Donald S. Grant, Robert F. Garry, Kristian G. Andersen, Juan Carlos de la Torre, Pardis C. Sabeti, John S. Schieffelin, and Michael B. A. Oldstone. Analysis of cd8+ t cell response during the 2013–2016 ebola epidemic in west africa. *Proceedings of the National Academy of Sciences*, 2018. ISSN 0027-8424. doi: 10.1073/pnas.1806200115. URL http://www.pnas.org/content/early/2018/07/17/1806200115.

[40] M.D. Selidji T. Agnandji, M.D. Angela Huttner, M.D. Madeleine E. Zinser, M.Med. Patricia Njuguna, Ph.D. Christine Dahlke, M.D. José F. Fernandes, M.Sc. Sabine Yerly, M.D. Julie-Anne Dayer, Ph.D. Verena Kraehling, Ph.D. Rahel Kasonta, Ph.D. Akim A. Adegnika, M.D., and Ph.D. Marcus Altfeld, M.D. Phase 1 trials of rvsv ebola vaccine in africa and europe. *The New England Journal of MedicineNew England*, 374:1647–1660, April

2016. doi: 10.1056/NEJMoa1502924. URL https://doi.org/10.1056/NEJMoa1502924.

[41] Alessandro Sette, John Sidney, Marie-France del Guercio, Scott Southwood, Jörg Ruppert, Carol Dahlberg, Howard M Grey, and Ralph T Kubo. Peptide binding to the most frequent hla-a class i alleles measured by quantitative molecular binding assays. *Molecular immunology*, 31(11):813–822, 1994. doi: https://doi.org/10.1016/0161-5890(94)90019-1.

[42] John Sidney, Jason Botten, Benjamin Neuman, Michael Buchmeier, and Alessandro Sette. Sars iedb entries. *IEDB*, 2006. URL https://www.iedb.org/reference/1000425.

[43] John Sidney, Scott Southwood, Carrie Moore, Carla Oseroff, Clemencia Pinilla, Howard M Grey, and Alessandro Sette. Measurement of mhc/peptide interactions by gel filtration or monoclonal antibody capture. *Current protocols in immunology*, 100(1):18–3, 2013. URL https://doi.org/10.1002/0471142735.im1803s100.

[44] S. Sridhar. Heterosubtypic t-cell immunity to influenza in humans: Challenges for universal t-cell influenza vaccines. *Front Immunol.*, 7(195), 2016. doi: doi: 10.3389/fimmu.2016.00195. URL https://doi.org/10.3389/fimmu.2016.00195.

[45] The International HIV Controllers Study et al. The major genetic determinants of hiv-1 control affect hla class i peptide presentation. *Science (New York, NY)*, 330(6010):1551, 2010. URL https://doi.org/10.1126/science.1195271.

[46] Nancy J. Sullivan, Anthony Sanchez, Pierre E. Rollin, Zhi yong Yang, and Gary J. Nabel. Development of a preventive vaccine for ebola virus infection in primates. *Nature*, 408:605–609, 2000. doi: 10.1038/35046108. URL https://doi.org/10.1038/35046108.

[47] C Sylvester-Hvid, Morten Nielsen, K Lamberth, G Røder, S Justesen, C Lundegaard, P Worning, H Thomadsen, O Lund, S Brunak, et al. Sars ctl vaccine candidateshla supertype, genome-wide scanning and biochemical validation. *Scandinavian Journal of Immunology*, 59(6):632–632, 2004. URL https://doi.org/10.1111/j.0001-2815.2004.00221.x.

[48] Yuki Takamatsu, Larissa Kolesnikova, and Stephan Becker. Ebola virus proteins np, vp35, and vp24 are essential and sufficient to mediate nucleocapsid transport. *Proceedings of the National Academy of Sciences*, 115(5): 1075–1080, 2018. URL https://doi.org/10.1073/pnas.1712263115.

[49] Thomas Trolle, Curtis P McMurtrey, John Sidney, Wilfried Bardet, Sean C Osborn, Thomas Kaever, Alessandro Sette, William H Hildebrand, Morten Nielsen, and Bjoern Peters. The length distribution of class i–restricted t cell epitopes is determined by both peptide supply and mhc allele–specific binding preference. *The Journal of Immunology*, 196(4):1480–1487, 2016. URL https://doi.org/10.4049/jimmunol.1501721.

[50] Yeou-Ping Tsao, Jian-Yu Lin, Jia-Tsrong Jan, Chih-Hsiang Leng, Chen-Chung Chu, Yuh-Cheng Yang, and Show-Li Chen. Hla-a 0201 t-cell epitopes in severe acute respiratory syndrome (sars) coronavirus nucleocapsid and spike proteins. *Biochemical and biophysical research communications*, 344(1):63–71, 2006. URL https://doi.org/10.1016/j.bbrc.2006.03.152.

[51] R Vita, JA Overton, JA Greenbaum, J Ponomarenko, JD Clark, JR Cantrell, DK Wheeler, JL Gabbard, D Hix, A Sette, and B Peters. The immune epitope database (iedb) 3.0. *Nucleic Acids Res.*, 2014.

[52] William Wan, Larissa Kolesnikova, Mairi Clarke, Alexander Koehler, Takeshi Noda, Stephan Becker, and John AG Briggs. Structure and assembly of the ebola virus nucleocapsid. *Nature*, 551(7680):394–397, 2017. URL https://doi.org/10.1038/nature24490.

[53] F Wang, T Ono, A Kalergis, W Zhang, T DiLorenzo, and K Lim. On the defing rules for interactions between the t cell receptor and its ligand: a critical role for a specific amino acid residue of the t cell receptor b chain. *Proc Natl Acad Sci USA*, 95(6), 1998. doi: 10.1073/pnas.95.9.5217.

[54] Kelly L. Warfield, John M. Dye, Jay B. Wells, Robert C. Unfer, Frederick W. Holtsberg, Sergey Shulenin, Hong Vu, Dana L. Swenso, Sina Bavari, and M. Javad Aman. Homologous and heterologous protection of nonhuman primates by ebola and sudan virus-like particles. *PLoS ONE*, 10(3):e0118881, March 2015. doi: 10.1371/journal.pone.0118881. URL https://doi.org/10.1371/journal.pone.0118881.

[55] K.L. Warfield, B.C. Bosio, C.M. Welcher, and E.M. Deal. Ebola virus-like particles protect from lethal ebola virus infection. *Proc. Natl. Acad. Sci.*, 100(26):15889–15894, 2003. doi: 10.1073/pnas.2237038100.

[56] P. Wauquier, N.and Becquart, C.; Padilla, S. Baize, and E.M. Leroy. Human fatal zaire ebola virus infection is associated with an aberrant innate immunity and with massive lymphocyte apoptosis. *Negl. Trop. Dis.*, 4 (e837), 2010. doi: doi: 10.1371/journal.pntd.0000837.

[57] JA Wilson and MK Hart. Protection from ebola virus mediated by cytotoxic t lymphocytes specific for the viral nucleoprotein. *J Virol*, 75 (6):2660–2664, 2001. doi: 10.1128/JVI.75.6.2660-2664.2001. URL https://doi.org/10.1128/JVI.75.6.2660-2664.2001.

[58] Guang Wu and Shaomin Yan. Reasoning of spike glycoproteins being more vulnerable to mutations among 158 coronavirus proteins from different species. *Journal of molecular modeling*, 11(1):8–16, 2005. URL https://doi.org/10.1007/s00894-004-0210-0.

[59] L Zhao, M Zhang, and H Cong. Advances in the study of hla-restricted epitope vaccines. *Human Vaccines and Immunotherapeutics*, 9:2566–2577, 2018. doi: 10.4161/hv.26088. URL https://doi.org/10.4161/hv.26088.

[60] Minghai Zhou, Dongping Xu, Xiaojuan Li, Hongtao Li, Ming Shan, Jiaren Tang, Min Wang, Fu-Sheng Wang, Xiaodong Zhu, Hua Tao, et al. Screening and identification of severe acute respiratory syndrome-associated coronavirus-specific ctl epitopes. *The Journal of Immunology*, 177(4):2138–2145, 2006. URL https://doi.org/10.4049/jimmunol.177.4.2138.

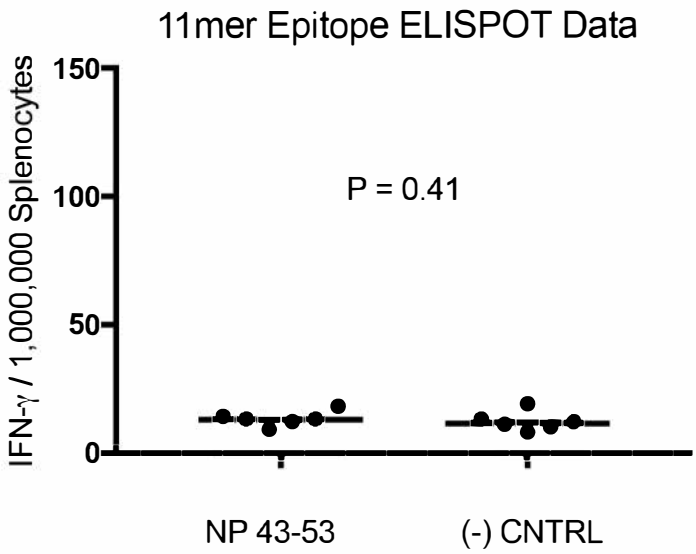


Figure 1: ELISPOT data from NP43-53 in 2mg of adjuvanted microspheres administered via intradermal (tail) injection showing the CTL response was not statistically different from (negative) control.

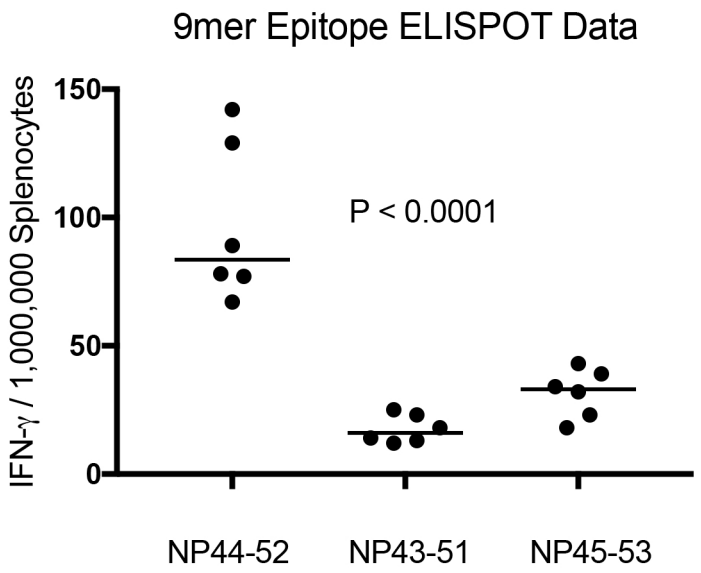


Figure 2: ELISPOT data from mice vaccinated with NP44-52 in 2mg of adjuvanted microspheres administered via intradermal (tail) injection was statistically different from the response after vaccination with NP43-51 and NP45-53.

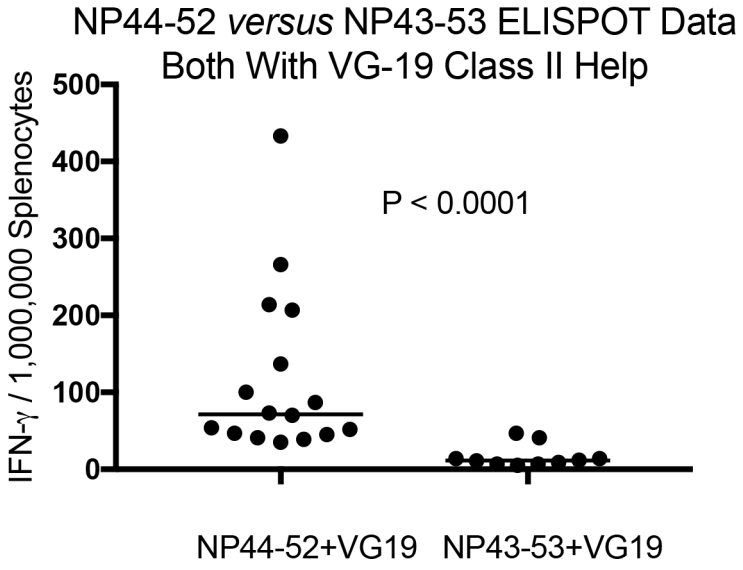


Figure 3: ELISPOT data from mice vaccinated with Class I peptides NP44-52 compared with NP43-53, each delivered adjuvanted microspheres adminstered via intradermal (tail) injection with with Class II help peptide VG19 in separate microspheres.

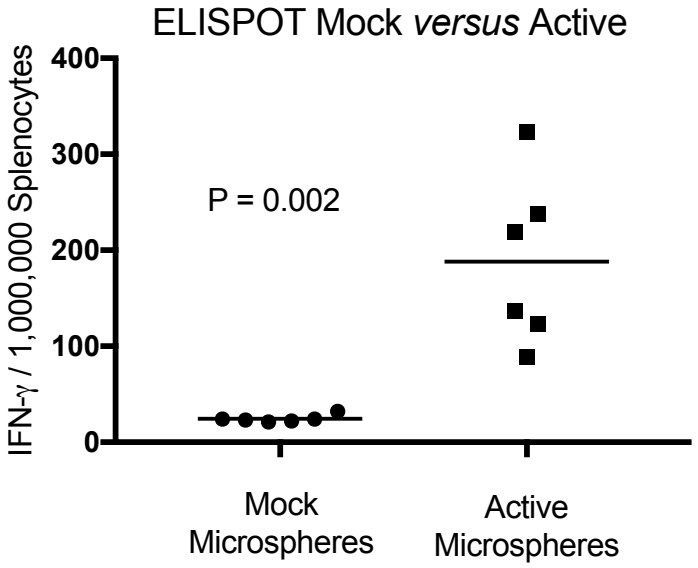


Figure 4: ELISPOT data from mice given a 20mg dose of mock microspheres (adjuvants only) via intraperitoneal injection or active microspheres (adjuvants and Class I peptide and active microspheres containing adjuvants and Class II peptide) and not exposed to EBOV.

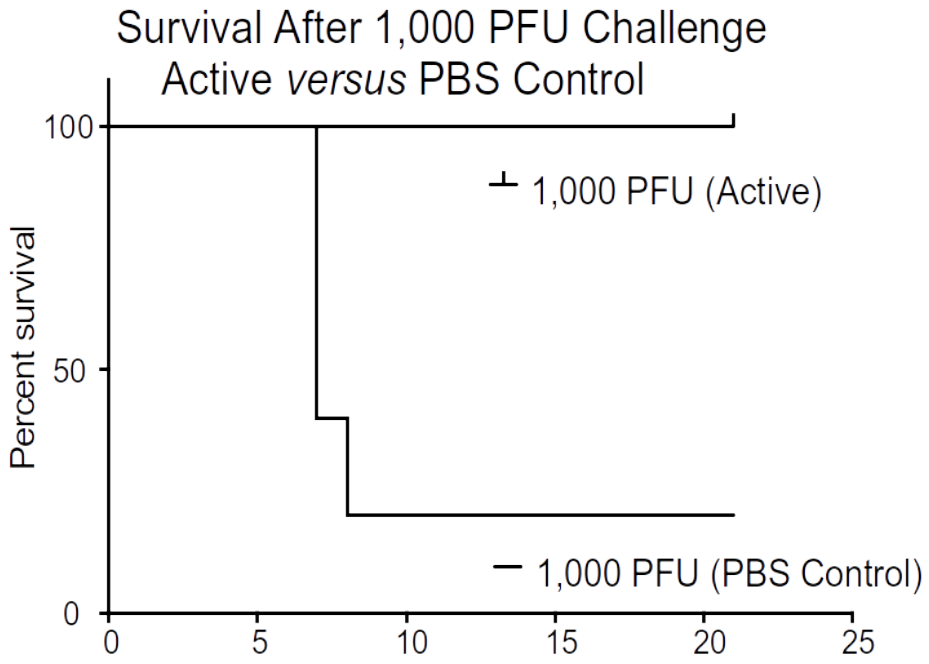


Figure 5: Post infection survival curves for 1,000 PFU challenged mice comparing mice vaccinated with microspheres containing the class I epitope sequence and different microspheres containing the class II epitope sequence versus PBS buffer control 14 days before maEBOV challenge. The difference between the number of survivors in the vaccinated group *versus* the PBS control group was statistically significant by chi square (P = 0.0003).

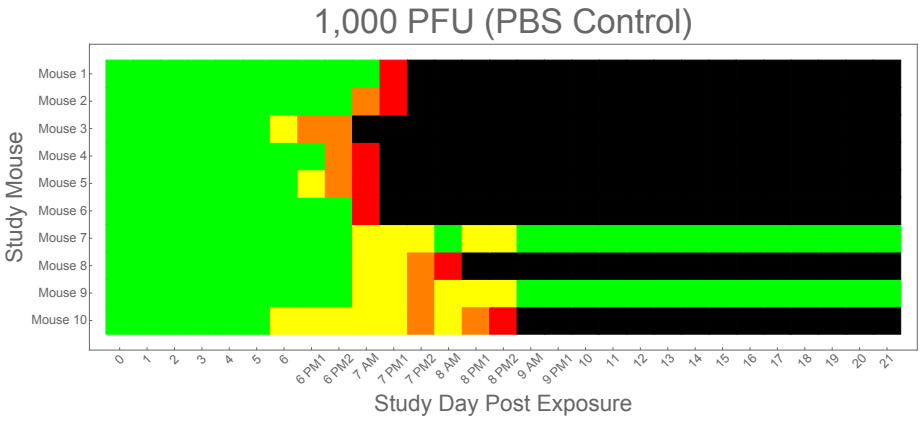


Figure 6: Clinical observations, scored from 1 (healthy) to 4 (moribund) made post infection in control animals receiving PBS buffer via intraperitoneal injection 14 days before infection. The clinical scores described in Table 3 are shown using the following color scheme: 1 = GREEN, 2 = YELLOW, 3 = ORANGE and 4 = RED. A dead mouse is coded in black. The frequency of measurements was increased on post infection days 6-9 coinciding with the anticipated period of peak morbidity.

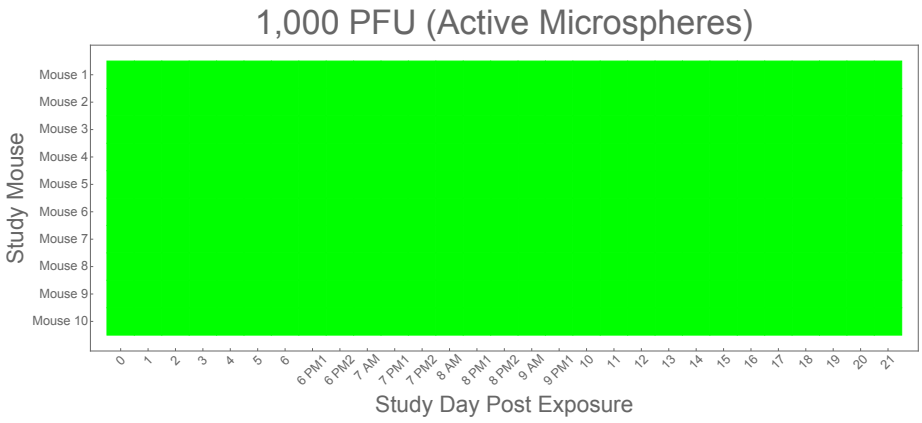


Figure 7: Clinical observations, scored from 1 (healthy) to 4 (moribund) made post infection in control animals receiving PBS buffer via intraperitoneal injection 14 days before infection. The clinical scores are shown using the following color scheme: 1 = GREEN, 2 = YELLOW, 3 = ORANGE and 4 = RED. All animals receiving the active vaccine remained healthy throughout the study. The frequency of measurements was increased on post infection days 6-9 coinciding with the anticipated period of peak morbidity.

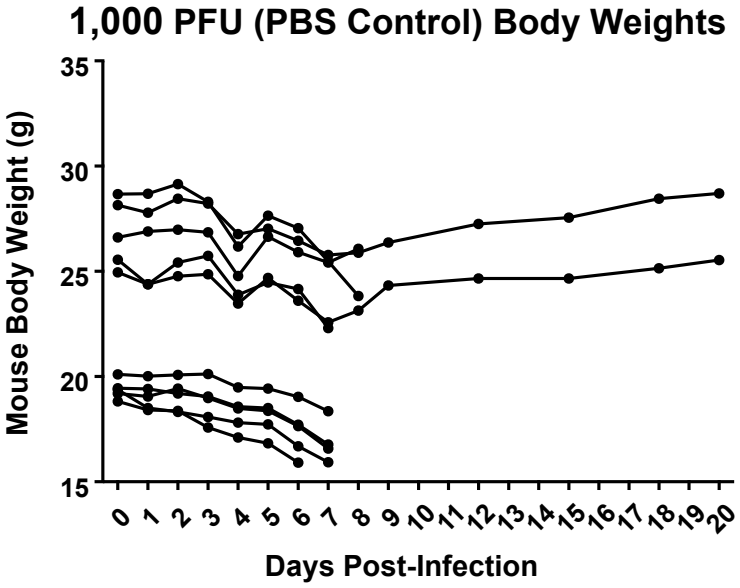


Figure 8: Daily weights were recorded post infection. Measurements for control animals, receiving PBS buffer 14 days before infection, are shown here.

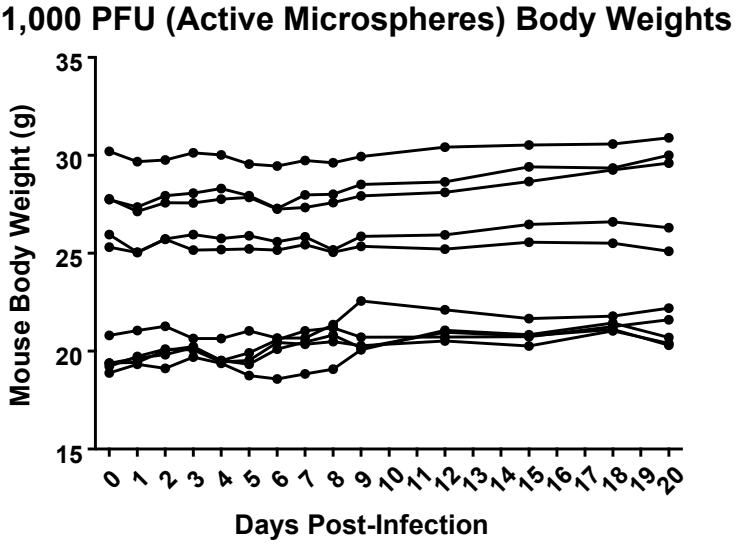


Figure 9: Daily weights were recorded post infection. Measurements for animals receiving active vaccine 14 days before infection, are shown here.

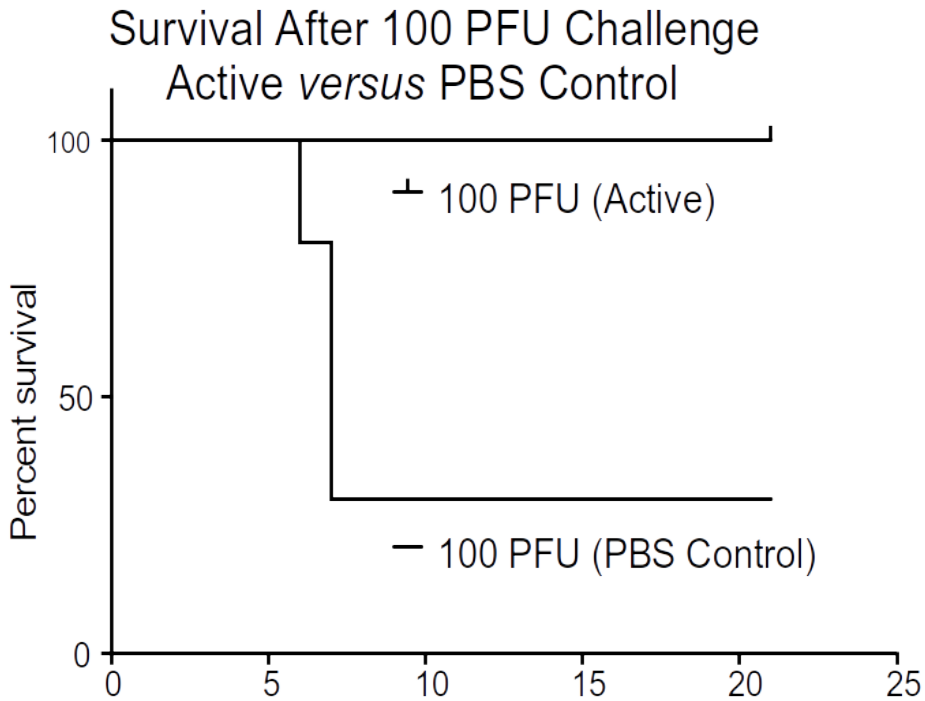


(a) Survival curve *versus* PBS buffer control. The difference between the number of survivors in the vaccinated group *versus* the PBS control group was statistically significant by chi square (P = 0.001).

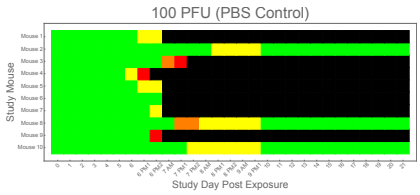


(b) Clinical observations (control).

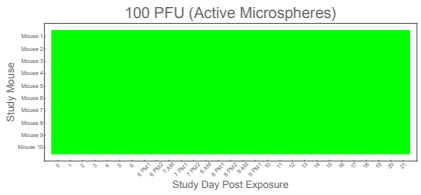


(c) Clinical observations (active).

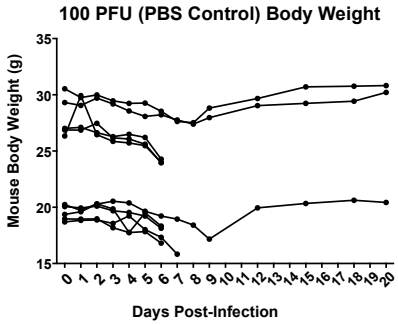


(d) Daily weights (control).

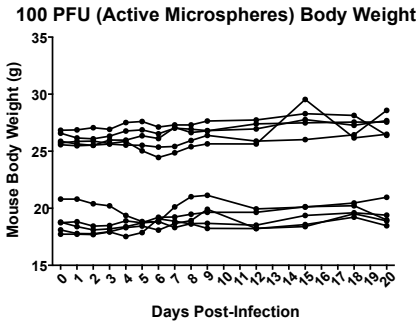


(e) Daily weights (active).

Figure 10: 100 PFU post-challenge data (active *versus* PBS buffer solution) collected beginning 14 days after vaccination.

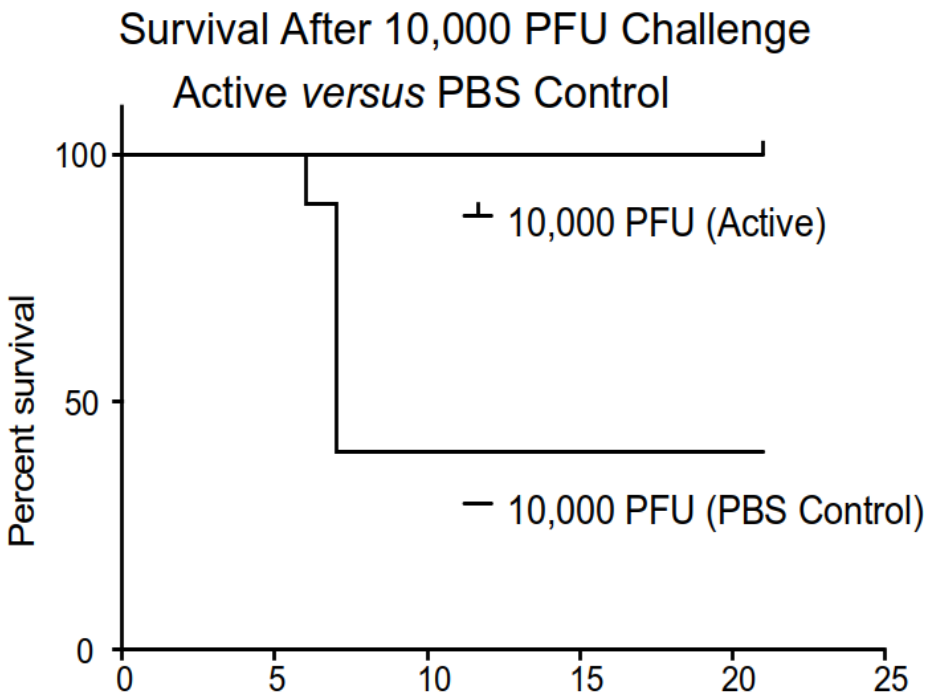


(a) Survival curve *versus* PBS buffer control. The difference between the number of survivors in the vaccinated group *versus* the PBS control group was statistically significant by chi square (P = 0.003).

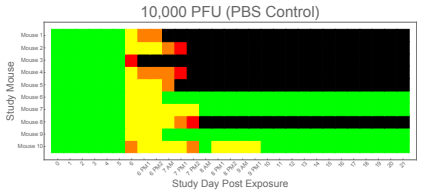


(b) Clinical observations (control).

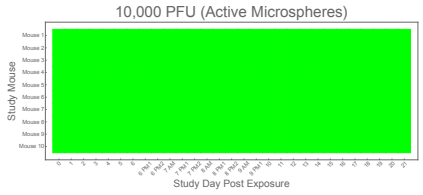


(c) Clinical observations (active).

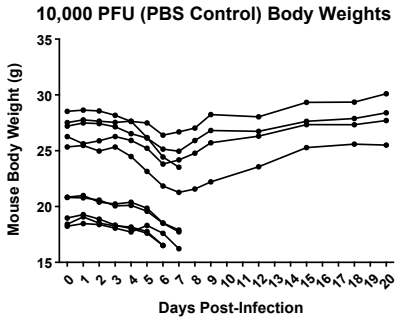


(d) Daily weights (control).

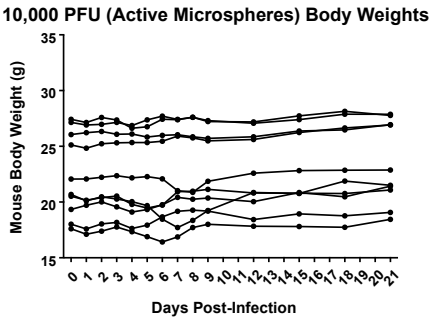


(e) Daily weights (active).

Figure 11: 10,000 PFU post-challenge data (active *versus* PBS buffer solution) collected beginning 14 days after vaccination.

```
CLUSTAL multiple sequence alignment by MUSCLE (3.8)

                                                                                  60
Sudan_EBOV_NP           MDKRVRGSWALGGQSEVDLDYHKILTAGLSVQQGIVRQRVIPVYVVSDLEGICQHIIQAF
Zaire_EBOV_NP           MDSRPQKIWMAPSLTESDMDYHKILTAGLSVQQGIVRQRVIPVYQVNNLEEICQLIIQAF
Bundibugyo_EBOV_NP      MDPRPIRTWMMHNTSEVEADYHKILTAGLSVQQGIVRQRIIPVYQISNLEEVCQLIIQAF
                        ** *    *   . :* : ********************:**** :.:** :** *****
```

Figure 12: NP44-52 has conserved residues across three strains of EBOV.

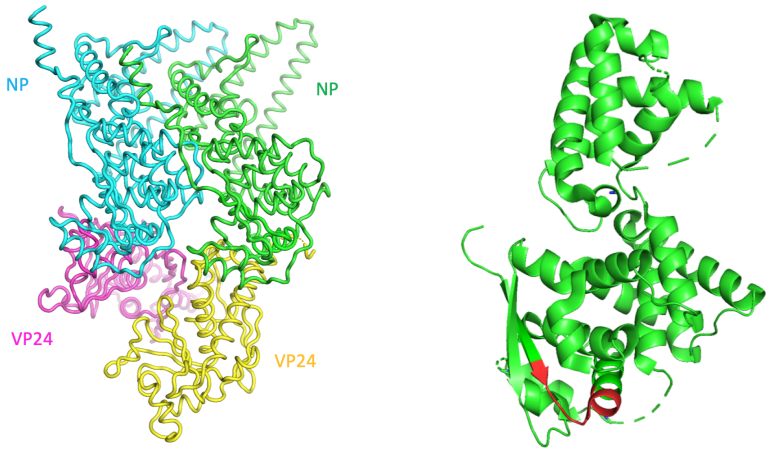


(a) EBOV nucleocapsid proteins NP and VP24 shown.

(b) NP44-52 is a conserved structural loop (red) buried inside the NP structure. The conservation and the location of NP44-52 suggest that residues 44-52 are important for the structural integrity of the EBOV NP.

Figure 13: The class I epitope used for this study is located within NP. Nucleocapsid proteins NP and VP24 are shown together in (a). A detailed view of NP with the study epitope position highlighted in shown in (b).

Cytokine / Survival Correlations for Control Groups

| Cytokine | p-Value | Correlation |
|---|---|---|
| Mo IL-6 | 0.050 | Decreased with survival |
| Mo MCP-1 | 0.019 | Decreased with Survival |
| Mo IL-9 | 0.015 | Increased with survival |
| Mo MIP-1b | 0.009 | Decreased with survival |
| Mo IL-12(p40) | 0.006 | Increased with Survival |
| Mo G-CSF | 0.005 | Decreased with Survival |
| Mo IL-1b | 0.005 | Increased with Survival |
| Mo IFN-g | 0.003 | Increased with Survival |
| Mo GM-CSF | 0.002 | Increased with Survival |
| Mo IL-12(p70) | 0.001 | Increased with Survival |
| Mo TNF-a | 0.001 | Increased with Survival |
| Mo IL-17 | 0.000 | Increased with Survival |
| Mo IL-10 | 0.000 | Decreased with Survival |

Table 4: Cytokines with statistically significant (positive or negative) correlation with survival in non-vaccinated mice are shown here along with (Pearson Correlation Analysis) p-values.

Computed HLA Binding Affinities for YQVNNLEEI

| Allele | Median $pIC_{50}nM$ | Consensus Score |
|---|---|---|
| **HLA-A*02:06** | 5.8 | 0.16 |
| **HLA-A*02:03** | 106 | 2.4 |
| **HLA-A*02:01** | 198 | 3.7 |
| | | |
| HLA-B*15:01 | 791 | 4.7 |
| HLA-A*23:01 | 1140 | 2.1 |
| HLA-B*40:01 | 1140 | 2.4 |
| HLA-A*68:02 | 5553 | 23 |
| HLA-A*24:02 | 5664 | 5.7 |
| HLA-B*53:01 | 8737 | 15 |
| HLA-B*58:01 | 12128 | 17 |
| HLA-B*51:01 | 13551 | 6.3 |
| HLA-A*26:01 | 15442 | 11 |
| HLA-A*32:01 | 17173 | 22 |
| HLA-B*44:03 | 18798 | 17 |
| HLA-B*35:01 | 19374 | 35 |
| HLA-A*30:01 | 23549 | 61 |
| HLA-B*44:02 | 27488 | 20 |
| HLA-A*30:02 | 31424 | 55 |

Table 5: Database-predicted HLA binding affinities for NP44-52 (YQVNNLEEI), the class I peptide used in this study.

Computed H-2 Binding Affinities for YQVNNLEEI

| Allele | Median $pIC_{50}nM$ | Consensus Score |
|---|---|---|
| **H-2-D$^{b}$** | 26 | 0.20 |
| | | |
| H-2-K$^{d}$ | 5639 | 7.0 |
| H-2-K$^{b}$ | 13722 | 32 |
| H-2-D$^{d}$ | 21052 | 23 |
| H-2-L$^{d}$ | - | 41 |

Table 6: Database-predicted H-2 binding affinities for NP44-52 (YQVNNLEEI), the class I peptide used in this study.

## Computed HLA-DR Binding Affinities for VKNEVNSFKAALSSLAKHG

| Allele | Start | 15-mer peptide | Median $pIC_{50}nM$ | Consensus Score |
|---|---|---|---|---|
| **HLA-DRB1*01:01** | 5 | VNSFKAALSSLAKHG | 4.1 | 0.28 |
| **HLA-DRB1*09:01** | 5 | VNSFKAALSSLAKHG | 6.0 | 0.010 |
| **HLA-DRB1*04:05** | 4 | EVNSFKAALSSLAKH | 14 | 0.19 |
| **HLA-DRB5*01:01** | 5 | VNSFKAALSSLAKHG | 24 | 1.8 |
| **HLA-DQA1*05:01/DQB1*03:01** | 3 | NEVNSFKAALSSLAK | 24 | 13 |
| **HLA-DRB1*04:01** | 5 | VNSFKAALSSLAKHG | 25 | 1.2 |
| **HLA-DPA1*02:01/DPB1*14:01** | 4 | EVNSFKAALSSLAKH | 27 | 4.7 |
| **HLA-DRB3*02:02** | 4 | EVNSFKAALSSLAKH | 27 | 0.080 |
| **HLA-DRB1*07:01** | 2 | KNEVNSFKAALSSLA | 40 | 4.7 |
| **HLA-DRB1*11:01** | 5 | VNSFKAALSSLAKHG | 66 | 4.3 |
| **HLA-DRB1*15:01** | 3 | NEVNSFKAALSSLAK | 152 | 3.4 |
| **HLA-DRB1*08:02** | 3 | NEVNSFKAALSSLAK | 162 | 1.4 |
| **HLA-DQA1*01:02/DQB1*06:02** | 3 | NEVNSFKAALSSLAK | 167 | 6.2 |
| **HLA-DPA1*02:01/DPB1*01:01** | 4 | EVNSFKAALSSLAKH | 401 | 26 |
| **HLA-DRB1*12:01** | 5 | VNSFKAALSSLAKHG | 769 | 8.8 |
| **HLA-DPA1*03:01/DPB1*04:02** | 4 | EVNSFKAALSSLAKH | 773 | 15 |
| **HLA-DRB4*01:01** | 3 | NEVNSFKAALSSLAK | 903 | 37 |
| | | | | |
| HLA-DRB1*13:02 | 1 | VKNEVNSFKAALSSL | 1380 | 28 |
| HLA-DRB1*03:01 | 2 | KNEVNSFKAALSSLA | 1498 | 13 |
| HLA-DQA1*03:01/DQB1*03:02 | 1 | VKNEVNSFKAALSSL | 1680 | 21 |
| HLA-DPA1*02:01/DPB1*05:01 | 5 | VNSFKAALSSLAKHG | 1811 | 25 |
| HLA-DQA1*04:01/DQB1*04:02 | 4 | EVNSFKAALSSLAKH | 1951 | 16 |
| HLA-DRB3*01:01 | 2 | KNEVNSFKAALSSLA | 1991 | 21 |
| HLA-DPA1*01:03/DPB1*02:01 | 4 | EVNSFKAALSSLAKH | 2002 | 26 |
| HLA-DPA1*01/DPB1*04:01 | 4 | EVNSFKAALSSLAKH | 2073 | 31 |
| HLA-DQA1*05:01/DQB1*02:01 | 2 | KNEVNSFKAALSSLA | 3341 | 32 |
| HLA-DQA1*01:01/DQB1*05:01 | 1 | VKNEVNSFKAALSSL | 3922 | 29 |

Table 7: Database-predicted HLA binding affinities for VKNEVNSFKAALSSLAKHG, the class II peptide used in this study.

Computed H2-I Binding Affinities for VKNEVNSFKAALSSLAKHG

| Allele | Start | 15-mer peptide | Median $pIC_{50}nM$ | Consensus Score |
|---|---|---|---|---|
| **H2-IA$^{b}$** | 4 | EVNSFKAALSSLAKH | 138 | 1.4 |
| H2-IA$^{d}$ | 5 | VNSFKAALSSLAKHG | 1069 | 6.1 |
| H2-IE$^{d}$ | 5 | VNSFKAALSSLAKHG | 5797 | 35 |

Table 8: Database-predicted H2-I binding affinities for VKNEVNSFKAALSSLAKHG, the class II peptide used in this study.

```
QHO62884          QASSRSSSRSRNSXRNSTPGSSRGTSPARMAGNGGDAALALLLLDRLNQLESKMSGKGQQ  240
QIC50514          QASSRSSSRSRNSSRNSTPGSNRGTSPARMAGNGGDAALALLLLDRLNQLESKMSGKGQQ  240
QIC50515          QASSRSSSRSRNSSRNSTPGSNRGTSPARMAGNGGDAALALLLLDRLNQLESKMSGKGQQ  240
QHZ00406          QASSRSSSRSRNSLRNSTPGSSRGTSPARMAGNGGDAALALLLLDRLNQLESKMSGKGQQ  240
QHW06046          QASSRSSSRSRNSLRNSTPGSSRGTSPARMAGNGGDAALALLLLDRLNQLESKMSGKGQQ  240
QHW06056          QASSRSSSRSRNSLRNSTPGSSRGTSPARMAGNGGDAALALLLLDRLNQLESKMSGKGQQ  240
QIA98602          QASSRSSSRSRNSSRNSTPGSSRGTSPARMAGNGGDAALALLLLDRLNQLESKMSGKGQQ  240
QIA20052          QASSRSSSRSRNSSRNSTPGSSRGTSPARMAGNGGDAALALLLLDRLNQLESKMSGKGQQ  240
QIA98613          QASSRSSSRSRNSSRNSTPGSSRGTSPARMAGNGGDAALALLLLDRLNQLESKMSGKGQQ  240
QHZ87599          QASSRSSSRSRNSSRNSTPGSSRGTSPARMAGNGGDAALALLLLDRLNQLESKMSGKGQQ  240
QHZ87589          QASSRSSSRSRNSSRNSTPGSSRGTSPARMAGNGGDAALALLLLDRLNQLESKMSGKGQQ  240
QHQ82471          QASSRSSSRSRNSSRNSTPGSSRGTSPARMAGNGGDAALALLLLDRLNQLESKMSGKGQQ  240
QHR63278          QASSRSSSRSRNSSRNSTPGSSRGTSPARMAGNGGDAALALLLLDRLNQLESKMSGKGQQ  240
QHR63258          QASSRSSSRSRNSSRNSTPGSSRGTSPARMAGNGGDAALALLLLDRLNQLESKMSGKGQQ  240
QHZ00365          QASSRSSSRSRNSSRNSTPGSSRGTSPARMAGNGGDAALALLLLDRLNQLESKMSGKGQQ  240
BCA25661          QASSRSSSRSRNSSRNSTPGSSRGTSPARMAGNGGDAALALLLLDRLNQLESKMSGKGQQ  240
QHZ00386          QASSRSSSRSRNSSRNSTPGSSRGTSPARMAGNGGDAALALLLLDRLNQLESKMSGKGQQ  240
QHZ00396          QASSRSSSRSRNSSRNSTPGSSRGTSPARMAGNGGDAALALLLLDRLNQLESKMSGKGQQ  240
BCA25671          QASSRSSSRSRNSSRNSTPGSSRGTSPARMAGNGGDAALALLLLDRLNQLESKMSGKGQQ  240
BCA25681          QASSRSSSRSRNSSRNSTPGSSRGTSPARMAGNGGDAALALLLLDRLNQLESKMSGKGQQ  240
QHU36851          QASSRSSSRSRNSSRNSTPGSSRGTSPARMAGNGGDAALALLLLDRLNQLESKMSGKGQQ  240
QHO62110          QASSRSSSRSRNSSRNSTPGSSRGTSPARMAGNGGDAALALLLLDRLNQLESKMSGKGQQ  240
QHQ71970          QASSRSSSRSRNSSRNSTPGSSRGTSPARMAGNGGDAALALLLLDRLNQLESKMSGKGQQ  240
QHO62115          QASSRSSSRSRNSSRNSTPGSSRGTSPARMAGNGGDAALALLLLDRLNQLESKMSGKGQQ  240
QHO60601          QASSRSSSRSRNSSRNSTPGSSRGTSPARMAGNGGDAALALLLLDRLNQLESKMSGKGQQ  240
QHU36871          QASSRSSSRSRNSSRNSTPGSSRGTSPARMAGNGGDAALALLLLDRLNQLESKMSGKGQQ  240
QHW06066          QASSRSSSRSRNSSRNSTPGSSRGTSPARMAGNGGDAALALLLLDRLNQLESKMSGKGQQ  240
QHN73817          QASSRSSSRSRNSSRNSTPGSSRGTSPARMAGNGGDAALALLLLDRLNQLESKMSGKGQQ  240
QHU79181          QASSRSSSRSRNSSRNSTPGSSRGTSPARMAGNGGDAALALLLLDRLNQLESKMSGKGQQ  240
QHU79201          QASSRSSSRSRNSSRNSTPGSSRGTSPARMAGNGGDAALALLLLDRLNQLESKMSGKGQQ  240
QHU36831          QASSRSSSRSRNSSRNSTPGSSRGTSPARMAGNGGDAALALLLLDRLNQLESKMSGKGQQ  240
QHU36841          QASSRSSSRSRNSSRNSTPGSSRGTSPARMAGNGGDAALALLLLDRLNQLESKMSGKGQQ  240
QHU36861          QASSRSSSRSRNSSRNSTPGSSRGTSPARMAGNGGDAALALLLLDRLNQLESKMSGKGQQ  240
QHU79211          QASSRSSSRSRNSSRNSTPGSSRGTSPARMAGNGGDAALALLLLDRLNQLESKMSGKGQQ  240
QIC50512          QASSRSSSRSRNSSRNSTPGSSRGTSPARMAGNGGDAALALLLLDRLNQLESKMSGKGQQ  240
QHR63288          QASSRSSSRSRNSSRNSTPGSSRGTSPARMAGNGGDAALALLLLDRLNQLESKMSGKGQQ  240
QIC50508          QASSRSSSRSRNSSRNSTPGSSRGTSPARMAGNGGDAALALLLLDRLNQLESKMSGKGQQ  240
QIC50513          QASSRSSSRSRNSSRNSTPGSSRGTSPARMAGNGGDAALALLLLDRLNQLESKMSGKGQQ  240
QIC50516          QASSRSSSRSRNSSRNSTPGSSRGTSPARMAGNGGDAALALLLLDRLNQLESKMSGKGQQ  240
QIC50507          QASSRSSSRSRNSSRNSTPGSSRGTSPARMAGNGGDAALALLLLDRLNQLESKMSGKGQQ  240
QIC50509          QASSRSSSRSRNSSRNSTPGSSRGTSPARMAGNGGDAALALLLLDRLNQLESKMSGKGQQ  240
QIC50511          QASSRSSSRSRNSSRNSTPGSSRGTSPARMAGNGGDAALALLLLDRLNQLESKMSGKGQQ  240
QHD43423          QASSRSSSRSRNSSRNSTPGSSRGTSPARMAGNGGDAALALLLLDRLNQLESKMSGKGQQ  240
QIB84680          QASSRSSSRSRNSSRNSTPGSSRGTSPARMAGNGGDAALALLLLDRLNQLESKMSGKGQQ  240
QIC50510          QASSRSSSRSRNSSRNSTPGSSRGTSPARMAGNGGDAALALLLLDRLNQLESKMSGKGQQ  240
QHQ71980          QASSRSSSRSRNSSRNSTPGSSRGTSPARMAGNGGDAALALLLLDRLNQLESKMSGKGQQ  240
QHN73802          QASSRSSSRSRNSSRNSTPGSSRGTSPARMAGNGGDAALALLLLDRLNQLESKMSGKGQQ  240
QHR84456          QASSRSSSRSRNSSRNSTPGSSRGTSPARMAGNGGDAALALLLLDRLNQLESKMSGKGQQ  240
QHR63298          QASSRSSSRSRNSSRNSTPGSSRGTSPARMAGNGGDAALALLLLDRLNQLESKMSGKGQQ  240
YP_009724397      QASSRSSSRSRNSSRNSTPGSSRGTSPARMAGNGGDAALALLLLDRLNQLESKMSGKGQQ  240
QHR63268          QASSRSSSRSRNSSRNSTPGSSRGTSPARMAGNGGDAALALLLLDRLNQLESKMSGKGQQ  240
QIC53221          QASSRSSSRSRNSSRNSTPGSSRGTSPARMAGNGGDAALALLLLDRLNQLESKMSGKGQQ  240
QIC53211          QASSRSSSRSRNSSRNSTPGSSRGTSPARMAGNGGDAALALLLLDRLNQLESKMSGKGQQ  240
BCA25651          QASSRSSSRSRNSSRNSTPGSSRGTSPARMAGNGGDAALALLLLDRLNQLESKMSGKGQQ  240
                  ************** *******.****************************************
```

Figure 14: Part 1 of 2. Sequences from 54 subjects with COVID-19 were found to have highly conserved nucleocapsid peptide sequences from positions 1-419 with the exception of three positions. At position 194, three individual sequences differ with non-conserved amino acid residues and one unknown amino acid. At position 202, a partially conserved amino acid variant is seen in two samples. At position 344, one non-conserved amino acid is present, however, this sample used a laboratory host cell line where only one of 4 replicates displayed this non-conserved amino acid substitution. These two mutation positions are colored according to the Clustal X color scheme.

```
QHO62884          WPQIAQFAPSASAFFGMSRIGMEVTPSGTWLTYTGAIKLDDKDPNFKDQVILLNKHIDAY  360
QIC50514          WPQIAQFAPSASAFFGMSRIGMEVTPSGTWLTYTGAIKLDDKDPNFKDQVILLNKHIDAY  360
QIC50515          WPQIAQFAPSASAFFGMSRIGMEVTPSGTWLTYTGAIKLDDKDPNFKDQVILLNKHIDAY  360
QHZ00406          WPQIAQFAPSASAFFGMSRIGMEVTPSGTWLTYTGAIKLDDKDPNFKDQVILLNKHIDAY  360
QHW06046          WPQIAQFAPSASAFFGMSRIGMEVTPSGTWLTYTGAIKLDDKDPNFKDQVILLNKHIDAY  360
QHW06056          WPQIAQFAPSASAFFGMSRIGMEVTPSGTWLTYTGAIKLDDKDPNFKDQVILLNKHIDAY  360
QIA98602          WPQIAQFAPSASAFFGMSRIGMEVTPSGTWLTYTGAIKLDDKDPNFKDQVILLNKHIDAY  360
QIA20052          WPQIAQFAPSASAFFGMSRIGMEVTPSGTWLTYTGAIKLDDKDPNFKDQVILLNKHIDAY  360
QIA98613          WPQIAQFAPSASAFFGMSRIGMEVTPSGTWLTYTGAIKLDDKDPNFKDQVILLNKHIDAY  360
QHZ87599          WPQIAQFAPSASAFFGMSRIGMEVTPSGTWLTYTGAIKLDDKDPNFKDQVILLNKHIDAY  360
QHZ87589          WPQIAQFAPSASAFFGMSRIGMEVTPSGTWLTYTGAIKLDDKDPNFKDQVILLNKHIDAY  360
QHQ82471          WPQIAQFAPSASAFFGMSRIGMEVTPSGTWLTYTGAIKLDDKDPNFKDQVILLNKHIDAY  360
QHR63278          WPQIAQFAPSASAFFGMSRIGMEVTPSGTWLTYTGAIKLDDKDPNFKDQVILLNKHIDAY  360
QHR63258          WPQIAQFAPSASAFFGMSRIGMEVTPSGTWLTYTGAIKLDDKDPNFKDQVILLNKHIDAY  360
QHZ00365          WPQIAQFAPSASAFFGMSRIGMEVTPSGTWLTYTGAIKLDDKDPNFKDQVILLNKHIDAY  360
BCA25661          WPQIAQFAPSASAFFGMSRIGMEVTPSGTWLTYTGAIKLDDKDPNFKDQVILLNKHIDAY  360
QHZ00386          WPQIAQFAPSASAFFGMSRIGMEVTPSGTWLTYTGAIKLDDKDPNFKDQVILLNKHIDAY  360
QHZ00396          WPQIAQFAPSASAFFGMSRIGMEVTPSGTWLTYTGAIKLDDKDPNFKDQVILLNKHIDAY  360
BCA25671          WPQIAQFAPSASAFFGMSRIGMEVTPSGTWLTYTGAIKLDDKDPNFKDQVILLNKHIDAY  360
BCA25681          WPQIAQFAPSASAFFGMSRIGMEVTPSGTWLTYTGAIKLDDKDPNFKDQVILLNKHIDAY  360
QHU36851          WPQIAQFAPSASAFFGMSRIGMEVTPSGTWLTYTGAIKLDDKDPNFKDQVILLNKHIDAY  360
QHO62110          WPQIAQFAPSASAFFGMSRIGMEVTPSGTWLTYTGAIKLDDKDPNFKDQVILLNKHIDAY  360
QHQ71970          WPQIAQFAPSASAFFGMSRIGMEVTPSGTWLTYTGAIKLDDKDPNFKDQVILLNKHIDAY  360
QHO62115          WPQIAQFAPSASAFFGMSRIGMEVTPSGTWLTYTGAIKLDDKDPNFKDQVILLNKHIDAY  360
QHO60601          WPQIAQFAPSASAFFGMSRIGMEVTPSGTWLTYTGAIKLDDKDPNFKDQVILLNKHIDAY  360
QHU36871          WPQIAQFAPSASAFFGMSRIGMEVTPSGTWLTYTGAIKLDDKDPNFKDQVILLNKHIDAY  360
QHW06066          WPQIAQFAPSASAFFGMSRIGMEVTPSGTWLTYTGAIKLDDKDPNFKDQVILLNKHIDAY  360
QHN73817          WPQIAQFAPSASAFFGMSRIGMEVTPSGTWLTYTGAIKLDDKDPNFKDQVILLNKHIDAY  360
QHU79181          WPQIAQFAPSASAFFGMSRIGMEVTPSGTWLTYTGAIKLDDKDPNFKDQVILLNKHIDAY  360
QHU79201          WPQIAQFAPSASAFFGMSRIGMEVTPSGTWLTYTGAIKLDDKDPNFKDQVILLNKHIDAY  360
QHU36831          WPQIAQFAPSASAFFGMSRIGMEVTPSGTWLTYTGAIKLDDKDPNFKDQVILLNKHIDAY  360
QHU36841          WPQIAQFAPSASAFFGMSRIGMEVTPSGTWLTYTGAIKLDDKDPNFKDQVILLNKHIDAY  360
QHU36861          WPQIAQFAPSASAFFGMSRIGMEVTPSGTWLTYTGAIKLDDKDPNFKDQVILLNKHIDAY  360
QHU79211          WPQIAQFAPSASAFFGMSRIGMEVTPSGTWLTYTGAIKLDDKDPNFKDQVILLNKHIDAY  360
QIC50512          WPQIAQFAPSASAFFGMSRIGMEVTPSGTWLTYTGAIKLDDKDPNFKDQVILLNKHIDAY  360
QHR63288          WPQIAQFAPSASAFFGMSRIGMEVTPSGTWLTYTGAIKLDDKDPNFKDQVILLNKHIDAY  360
QIC50508          WPQIAQFAPSASAFFGMSRIGMEVTPSGTWLTYTGAIKLDDKDPNFKDQVILLNKHIDAY  360
QIC50513          WPQIAQFAPSASAFFGMSRIGMEVTPSGTWLTYTGAIKLDDKDPNFKDQVILLNKHIDAY  360
QIC50516          WPQIAQFAPSASAFFGMSRIGMEVTPSGTWLTYTGAIKLDDKDPNFKDQVILLNKHIDAY  360
QIC50507          WPQIAQFAPSASAFFGMSRIGMEVTPSGTWLTYTGAIKLDDKDPNFKDQVILLNKHIDAY  360
QIC50509          WPQIAQFAPSASAFFGMSRIGMEVTPSGTWLTYTGAIKLDDKDPNFKDQVILLNKHIDAY  360
QIC50511          WPQIAQFAPSASAFFGMSRIGMEVTPSGTWLTYTGAIKLDDKDPNFKDQVILLNKHIDAY  360
QHD43423          WPQIAQFAPSASAFFGMSRIGMEVTPSGTWLTYTGAIKLDDKDPNFKDQVILLNKHIDAY  360
QIB84680          WPQIAQFAPSASAFFGMSRIGMEVTPSGTWLTYTGAIKLDDKDPNFKDQVILLNKHIDAY  360
QIC50510          WPQIAQFAPSASAFFGMSRIGMEVTPSGTWLTYTGAIKLDDKDPNFKDQVILLNKHIDAY  360
QHQ71980          WPQIAQFAPSASAFFGMSRIGMEVTPSGTWLTYTGAIKLDDKDPNFKDQVILLNKHIDAY  360
QHN73802          WPQIAQFAPSASAFFGMSRIGMEVTPSGTWLTYTGAIKLDDKDPNFKDQVILLNKHIDAY  360
QHR84456          WPQIAQFAPSASAFFGMSRIGMEVTPSGTWLTYTGAIKLDDKDPNFKDQVILLNKHIDAY  360
QHR63298          WPQIAQFAPSASAFFGMSRIGMEVTPSGTWLTYTGAIKLDDKDPNFKDQVILLNKHIDAY  360
YP_009724397      WPQIAQFAPSASAFFGMSRIGMEVTPSGTWLTYTGAIKLDDKDPNFKDQVILLNKHIDAY  360
QHR63268          WPQIAQFAPSASAFFGMSRIGMEVTPSGTWLTYTGAIKLDDKDPNFKDQVILLNKHIDAY  360
QIC53221          WPQIAQFAPSASAFFGMSRIGMEVTPSGTWLTYTGAIKLDDKDPNFKDQVILLNKHIDAY  360
QIC53211          WPQIAQFAPSASAFFGMSRIGMEVTPSGTWLTYTGAIKLDDKDPNFKDQVILLNKHIDAY  360
BCA25651          WPQIAQFAPSASAFFGMSRIGMEVTPSGTWLTYTGAIKLDDKDSNFKDQVILLNKHIDAY  360
                  ******************************************** ****************
```

Figure 15: Part 2 of 2. Sequences from 54 subjects with COVID-19 were found to have highly conserved nucleocapsid peptide sequences from positions 1-419 with the exception of three positions. At position 194, three individual sequences differ with non-conserved amino acid residues and one unknown amino acid. At position 202, a partially conserved amino acid variant is seen in two samples. At position 344, one non-conserved amino acid is present, however, this sample used a laboratory host cell line where only one of 4 replicates displayed this non-conserved amino acid substitution. These two mutation positions are colored according to the Clustal X color scheme.

COVID-19 nucleocapsid peptides with associated predicted HLA restricted binding affinities (1/4)

| Peptide | Start Position | Allele | NetMHC 4.0 $pIC_{50}$nM | NetMHCpan 4.0 $pIC_{50}$nM | SARS Same? |
|---|---|---|---|---|---|
| LSPRWYFYY | 104 | HLA-A*01:01 | 48.64 | 76.9 | YES |
| LLLDRLNQL | 222 | HLA-A*02:01 | 14.81 | 11.3 | YES |
| GMSRIGMEV | 316 | HLA-A*02:01 | 50.61 | 48.1 | YES |
| KTFPPTEPK | 361 | HLA-A*03:01 | 20.8 | 18.8 | YES |
| KSAAEASKK | 249 | HLA-A*03:01 | 116.22 | 139.4 | YES |
| LIRQGTDYK | 291 | HLA-A*03:01 | 274.69 | 137.5 | YES |
| ASAFFGMSR | 311 | HLA-A*03:01 | 292.41 | 285.3 | YES |
| QLESKMSGK | 229 | HLA-A*03:01 | 322.41 | 751 | NO |
| FTALTQHGK | 53 | HLA-A*03:01 | 788.84 | 345.5 | YES |
| KTFPPTEPK | 361 | HLA-A*11:01 | 6.28 | 7.7 | YES |
| ASAFFGMSR | 311 | HLA-A*11:01 | 14.4 | 15.3 | YES |
| FTALTQHGK | 53 | HLA-A*11:01 | 127.28 | 44.9 | YES |
| KSAAEASKK | 249 | HLA-A*11:01 | 76.73 | 62.2 | YES |
| AGLPYGANK | 119 | HLA-A*11:01 | 240.23 | 157.5 | NO |
| LIRQGTDYK | 291 | HLA-A*11:01 | 984.82 | 160.6 | YES |
| LSPRWYFYY | 104 | HLA-A*11:01 | 253.34 | 492.8 | YES |
| TQALPQRQK | 379 | HLA-A*11:01 | 740.66 | 415.1 | NO |
| QQQGQTVTK | 240 | HLA-A*11:01 | 428.26 | 470.3 | YES |
| KHIDAYKTF | 355 | HLA-A*23:01 | 134.12 | 778.7 | YES |
| YYRRATRRI | 86 | HLA-A*23:01 | 151.38 | 366.6 | NO |
| TWLTYTGAI | 329 | HLA-A*23:01 | 24164.38 | 282.1 | NO |
| KHWPQIAQF | 299 | HLA-A*23:01 | 317.71 | 313.7 | YES |
| KAYNVTQAF | 266 | HLA-A*23:01 | 341.14 | 602.3 | NO |
| YYRRATRRI | 86 | HLA-A*24:02 | 74.89 | 322 | NO |

Table 9: This set of 53 unique peptides (part 1 of 4) achieves > 95% world-wide population coverage. The starting position is within the Nucleocapsid. Peptides chosen with binding affinity predictions less than 500nm via NetMHC 4.0 or NetMHCpan 4.0. Peptide sequences colored in red have literature references as known *in-vitro* binders to the predicted allele match (see text).

COVID-19 nucleocapsid peptides with associated predicted HLA restricted binding affinities (2/4)

| Peptide | Start Position | Allele | NetMHC 4.0 $pIC_{50}$nM | NetMHCpan 4.0 $pIC_{50}$nM | SARS Same? |
|---|---|---|---|---|---|
| FAPSASAFF | 307 | HLA-A*24:02 | 422.31 | 847.7 | YES |
| NTASWFTAL | 48 | HLA-A*26:01 | 1113.04 | 122.6 | YES |
| ELIRQGTDY | 290 | HLA-A*26:01 | 652.8 | 327.8 | NO |
| FAPSASAFF | 307 | HLA-A*26:01 | 349.57 | 606.6 | YES |
| IGYYRRATR | 84 | HLA-A*33:03 | N/A | 57.8 | YES |
| NVTQAFGRR | 269 | HLA-A*33:03 | N/A | 62.5 | YES |
| ASAFFGMSR | 311 | HLA-A*33:03 | N/A | 149.3 | YES |
| QASSRSSSR | 181 | HLA-A*33:03 | N/A | 163.9 | YES |
| YNVTQAFGR | 268 | HLA-A*33:03 | N/A | 189.1 | YES |
| GYYRRATRR | 85 | HLA-A*33:03 | N/A | 359.4 | YES |
| SSRSSSRSR | 183 | HLA-A*33:03 | N/A | 395.3 | YES |
| FPRGQGVPI | 66 | HLA-B*07:02 | 3.82 | 4.7 | YES |
| KPRQKRTAT | 257 | HLA-B*07:02 | 4.42 | 18.8 | YES |
| SPRWYFYYL | 105 | HLA-B*07:02 | 6.32 | 15.3 | YES |
| RIRGGDGKM | 93 | HLA-B*07:02 | 149.86 | 173 | NO |
| NPANNAAIV | 150 | HLA-B*07:02 | 184.8 | 569.3 | NO |
| LPNNTASWF | 45 | HLA-B*07:02 | 244.3 | 334 | YES |
| SPRWYFYYL | 105 | HLA-B*08:01 | 13.77 | 42.1 | YES |
| LLLDRLNQL | 222 | HLA-B*08:01 | 125.72 | 136.8 | YES |
| FPRGQGVPI | 66 | HLA-B*08:01 | 245.35 | 368.3 | YES |
| KPRQKRTAT | 257 | HLA-B*08:01 | 364.72 | 432.6 | YES |
| KAYNVTQAF | 266 | HLA-B*15:01 | 40.35 | 19 | NO |
| LLNKHIDAY | 352 | HLA-B*15:01 | 33.04 | 32.5 | YES |

Table 10: This set of 53 unique peptides (part 2 of 4) achieves > 95% world-wide population coverage. The starting position is within the Nucleocapsid. Peptides chosen with binding affinity predictions less than 500nm via NetMHC 4.0 or NetMHCpan 4.0. Peptide sequences colored in red have literature references as known *in-vitro* binders to the predicted allele match (see text).

COVID-19 nucleocapsid peptides with associated predicted HLA restricted binding affinities (3/4)

| Peptide | Start Position | Allele | NetMHC 4.0 $pIC_{50}$nM | NetMHCpan 4.0 $pIC_{50}$nM | SARS Same? |
|---|---|---|---|---|---|
| LQLPQGTTL | 159 | HLA-B*15:01 | 105.55 | 229.8 | YES |
| FAPSASAFF | 307 | HLA-B*15:01 | 213.11 | 281.9 | YES |
| FSKQLQQSM | 403 | HLA-B*15:01 | 219.07 | 286 | NO |
| RLNQLESKM | 226 | HLA-B*15:01 | 1496.11 | 490.3 | NO |
| QFAPSASAF | 306 | HLA-B*15:01 | 493.85 | 700.3 | YES |
| RRIRGGDGK | 92 | HLA-B*27:05 | 65.94 | 72.5 | NO |
| RRATRRIRG | 88 | HLA-B*27:05 | 253.64 | 787.8 | NO |
| QRNAPRITF | 9 | HLA-B*27:05 | 560.56 | 262.1 | NO |
| YRRATRRIR | 87 | HLA-B*27:05 | 415.31 | 597.7 | NO |
| NTASWFTAL | 48 | HLA-B*39:01 | 47.87 | 353.3 | YES |
| KKADETQAL | 374 | HLA-B*39:01 | 137.43 | 926.4 | NO |
| LQLPQGTTL | 159 | HLA-B*39:01 | 238.19 | 228.7 | YES |
| TRNPANNAA | 148 | HLA-B*39:01 | 406.62 | 818.3 | NO |
| MEVTPSGTW | 322 | HLA-B*44:02 | 11.48 | 14.2 | YES |
| LPNNTASWF | 45 | HLA-B*53:01 | 19.03 | 25.7 | YES |
| TPSGTWLTY | 325 | HLA-B*53:01 | 26.99 | 79 | YES |
| LPAADLDDF | 395 | HLA-B*53:01 | 193.75 | 74.8 | NO |
| FAPSASAFF | 307 | HLA-B*53:01 | 1164.6 | 317.4 | YES |
| GANKDGIIW | 124 | HLA-B*53:01 | 320.56 | 1015.8 | NO |
| KAYNVTQAF | 266 | HLA-B*58:01 | 12.51 | 17.7 | NO |
| GANKDGIIW | 124 | HLA-B*58:01 | 158.07 | 35.3 | NO |
| KMKDLSPRW | 100 | HLA-B*58:01 | 83.99 | 99.2 | NO |
| LSPRWYFYY | 104 | HLA-B*58:01 | 359.42 | 430.6 | YES |
| KAYNVTQAF | 266 | HLA-C*03:04 | N/A | 12.7 | NO |

Table 11: This set of 53 unique peptides (part 3 of 4) achieves > 95% world-wide population coverage. The starting position is within the Nucleocapsid. Peptides chosen with binding affinity predictions less than 500nm via NetMHC 4.0 or NetMHCpan 4.0. Peptide sequences colored in red have literature references as known *in-vitro* binders to the predicted allele match (see text).

COVID-19 nucleocapsid peptides with associated predicted HLA restricted binding affinities (4/4)

| Peptide | Start Position | Allele | NetMHC 4.0 $pIC_{50}nM$ | NetMHCpan 4.0 $pIC_{50}nM$ | SARS Same? |
|---|---|---|---|---|---|
| FAPSASAFF | 307 | HLA-C*03:04 | N/A | 41.4 | YES |
| LTYTGAIKL | 331 | HLA-C*03:04 | N/A | 44.8 | NO |
| NTASWFTAL | 48 | HLA-C*03:04 | N/A | 58.8 | YES |
| SAFFGMSRI | 312 | HLA-C*03:04 | N/A | 68 | YES |
| LQLPQGTTL | 159 | HLA-C*03:04 | N/A | 99.5 | YES |
| FSKQLQQSM | 403 | HLA-C*03:04 | N/A | 149.9 | NO |
| FPRGQGVPI | 66 | HLA-C*03:04 | N/A | 434.9 | YES |
| YRRATRRIR | 87 | HLA-C*07:01 | 112.27 | 8786.2 | NO |
| QRNAPRITF | 9 | HLA-C*07:01 | 1337.36 | 198.9 | NO |
| YYRRATRRI | 86 | HLA-C*07:01 | 254.32 | 957.2 | NO |
| LKFPRGQGV | 64 | HLA-C*07:01 | 446.18 | 1633.3 | NO |
| QRNAPRITF | 9 | HLA-C*07:02 | 261.17 | 237.8 | NO |
| YYRRATRRI | 86 | HLA-C*07:02 | 6229.2 | 242.2 | NO |
| FAPSASAFF | 307 | HLA-C*07:02 | 16893.5 | 347.4 | YES |
| KHWPQIAQF | 299 | HLA-C*07:02 | 430.68 | 971.3 | YES |
| NFKDQVILL | 345 | HLA-C*07:02 | 29905.43 | 462.1 | NO |
| KAYNVTQAF | 266 | HLA-C*07:02 | 668.01 | 477 | NO |
| FAPSASAFF | 307 | HLA-C*08:01 | N/A | 280.1 | YES |
| KAYNVTQAF | 266 | HLA-C*08:01 | N/A | 412.2 | NO |

Table 12: This set of 53 unique peptides (part 4 of 4) achieves $> 95\%$ world-wide population coverage. The starting position is within the Nucleocapsid. Peptides chosen with binding affinity predictions less than 500nm via NetMHC 4.0 or NetMHCpan 4.0. Peptide sequences colored in red have literature references as known *in-vitro* binders to the predicted allele match (see text).

COVID-19 nucleocapsid top candidate peptides with associated predicted HLA restricted binding affinities

| Peptide | Start Position | Allele | NetMHC 4.0 $pIC_{50}nM$ | NetMHCpan 4.0 $pIC_{50}nM$ | SARS Same? |
|---|---|---|---|---|---|
| LSPRWYFYY | 104 | HLA-A*01:01 | 48.64 | 76.9 | YES |
| LLLDRLNQL | 222 | HLA-A*02:01 | 14.81 | 11.3 | YES |
| KTFPPTEPK | 361 | HLA-A*03:01 | 20.8 | 18.8 | YES |
| KTFPPTEPK | 361 | HLA-A*11:01 | 6.8 | 7.7 | YES |
| KHIDAYKTF | 355 | HLA-A*23:01 | 134.12 | 778.7 | YES |
| YYRRATRRI | 86 | HLA-A*24:02 | 74.89 | 322 | NO |
| NTASWFTAL | 48 | HLA-A*26:01 | 1113.04 | 122.6 | YES |
| IGYYRRATR | 84 | HLA-A*33:03 | N/A | 57.8 | YES |
| FPRGQGVPI | 66 | HLA-B*07:02 | 3.82 | 4.7 | YES |
| SPRWYFYYL | 105 | HLA-B*08:01 | 13.77 | 42.1 | YES |
| KAYNVTQAF | 266 | HLA-B*15:01 | 40.35 | 19 | NO |
| RRIRGGDGK | 92 | HLA-B*27:05 | 65.94 | 72.5 | NO |
| NTASWFTAL | 48 | HLA-B*39:01 | 47.87 | 353.3 | YES |
| MEVTPSGTW | 322 | HLA-B*44:02 | 11.48 | 14.2 | YES |
| LPNNTASWF | 45 | HLA-B*53:01 | 19.03 | 25.7 | YES |
| KAYNVTQAF | 266 | HLA-B*58:01 | 12.51 | 17.7 | NO |
| KAYNVTQAF | 266 | HLA-C*03:04 | N/A | 12.7 | NO |
| YRRATRRIR | 87 | HLA-C*07:01 | 112.27 | 8786.2 | NO |
| QRNAPRITF | 9 | HLA-C*07:02 | 112.27 | 237.8 | NO |
| FAPSASAFF | 307 | HLA-C*08:01 | N/A | 280.1 | YES |

Table 13: This set of 16 unique peptides represents the minimum number required to achieve $> 95\%$ world-wide population coverage. The starting position is within the Nucleocapsid. Top binding affinity predictions chosen via NetMHC 4.0 or NetMHCpan 4.0. Peptide sequences colored in red have literature references as known *in-vitro* binders to the predicted allele match (see text).

## Projected World-Wide Population Coverage for a COVID-19 Peptide Vaccine Targeting 9mer Peptides on Nucleocapsid Proteins

| Minimum Epitope Matches / Allele / Person | % Projected Coverage | Cumulative % Population Coverage |
|---|---|---|
| 1 | 18.14 | 97.27 |
| 2 | 35.05 | 79.13 |
| 3 | 29.7 | 44.08 |
| 4 | 12.02 | 14.37 |
| 5 | 2.2 | 2.35 |
| 6 | 0.15 | 0.15 |

Table 14: Data showing projected HLA world-wide population coverage for a COVID-19 vaccine using the 16 epitopes listed in Table 13. If we assume a least one HLA match per peptide capable of producing a clinically relevant immune response in a person, we can achieve 97.27% global population coverage with a 16 class I peptide CTL vaccine.

## Projected China-Specific Population Coverage for a COVID-19 Peptide Vaccine Targeting 9mer Peptides on Nucleocapsid Proteins

| Minimum Epitope Matches / Allele / Person | % Projected Coverage | Cumulative % Population Coverage |
|---|---|---|
| 1 | 26.02 | 94.39 |
| 2 | 38.01 | 68.37 |
| 3 | 23.14 | 30.36 |
| 4 | 6.42 | 7.22 |
| 5 | 0.77 | 0.8 |
| 6 | 0.03 | 0.03 |

Table 15: If we take the assumptions made in the global projected population coverage Table 14 now assuming a China-specific HLA distribution, we still can achieve 94.39% population coverage